CHARGE EXCHANGE SCATTERING OF PROTONS ON DEUTERONS

by

David R. Firth, M.A.

A thesis submitted in partial fulfilment of the requirements for the degree of Doctor of Philosophy in the Faculty of Graduate Studies and Research at McGill University

Radiation Laboratory
December, 1959.

David R. Firth CHARGE EXCHANGE SCATTERING OF PROTONS ON DEUTERONS

A diffusion cloud chamber and its ancillary equipment were constructed and used to investigate the energy spectrum of fast neutrons produced by bombarding deuterium in the chamber with 85 Mev protons.

Reasons are adduced to show that these fast neutrons are the result of an exchange collision caused by a Heisenberg type of force in which the spins of the nucleons are also exchanged.

There is, however, disagreement with the calculations of Gluckstern and Bethe, who predicted a much narrower energy spectrum for the fast neutrons than we found by experiment. We suggest reasons for the discrepancy.

<u>ACKNOWLEDGEMENTS</u>

The author would like warmly to thank Dr. J. S. Foster, F.R.S., for his vital help in this work, and for his constant kindness.

Dr. R. P. Shutt of Brookhaven National Laboratory very generously loaned some of the equipment and extended the loan for three years, far beyond the expected period.

Sincere thanks are also due to those other members of the Radiation Laboratory who helped directly or by encouragement, and in particular to Mr. S. Doig of the machine shop.

CONTENTS

SUMMARY	Page
SUMMARY	
ACKNOWLEDGEMENTS	
INTRODUCTION	1
DEUTERIUM PREPARATION	6
THE DIFFUSION CLOUD CHAMBER	11
WORKING OF EQUIPMENT AND CYCLOTRON RUNS	25
MEASUREMENT OF TRACKS	36
KINEMATICAL CALCULATIONS	48
RESULTS AND DISCUSSION	52
REFERENCES	61
APPENDIX A	(i)
APPENDIX B	(vii)
APPENDIX C	(xi)

INTRODUCTION

This is a report on some experiments in which 90 Mev protons knock neutrons from deuterium gas in a diffusion chamber at a pressure of 20 atmospheres. Numerous pairs of low energy tracks formed by the remaining protons invite the interpretation that these proton pairs are left in a $\ell=0$ state, and consequently support the Heisenberg forces with spin exchange in accord with Paulits exclusion principle (Firth, 1959). (For examples of slow proton pairs, see Figures 11 and 12.)

At the same time, however, the distribution in energy of fast neutrons far exceeds the range expected in theory (Gluckstern and Bethe, 1951), and thus indicates that existing theory is not sufficient. Many events with high energy protons are clearly not included in the above interpretation, and these form the subject of a later discussion.

The above implies the assumption that, following the collision, the two slow protons are commonly left in the &=0 state; other possible states will be discussed later.

The existence of charge exchange forces between nucleons was shown by the production of fast protons when hydrogen is bombarded by neutrons having an energy much greater than the depth of the potential well between the nucleons (Fermi, 1950). Charge exchange forces are usually divided into the Majorana force in which nuclear spins are not exchanged, and the Heisenberg force with exchange of spin as well as space co-ordinates in the potential function. It is not possible (at least if one ignores non-central forces) to find out from n-p single scattering experiments whether or not the spin is exchanged.

We may picture the process studied here as the exchange of charge

between the incident proton and the neutron in the deuteron, whilst the proton in the deuteron moves with a momentum typical for the deuteron and separated from the region of the exchange process by a distance whose average is of the order of the deuteron radius. A fast neutron carries on its way. After this exchange process has occurred, the two protons must not be left in an impossible situation, such as a symmetric state, for they are Fermi-Dirac particles.

In visualising these nuclear processes in terms of either waves or particles, it is useful to have some idea of the dimensions involved; in units of 10^{-12} cm the wavelength of a 100 MeV proton is 0.3, the range of nuclear forces is thought to be about 20 and the radius of the deuteron about 40.

According to quantum mechanics, the nature of the final state has as much influence on the rate of reaction as the initial state, and in particular this reaction will go more easily into states in which the two slow protons have $\ell=0$, than into states with $\ell=1$. This is because the wave function for $\ell=1$, at distances of the deuteron average radius and below 5 MeV, is small compared with the $\ell=0$ wave function.

However, by the Pauli principle, & = 0 implies a singlet spin state, whereas the deuteron is a triplet state, so that in exchanging the charge, the spin of the exchanging nucleon in the deuteron must be flipped. So if the reaction happens easily, with a relatively high production of low energy proton pairs, one can conclude that a Heisenberg force is present.

Calculations on the neutron-deuteron reactions at 90 Mev have been done by Chew (1950, 1951) and by Gluckstern and Bethe (1951) (hereafter known as "G-B"). The apparently arbitrary separation into a fast

primary exchange interaction and a final state interaction between just two slow particles is analysed in detail by Watson (1952) and by Migdal (1955).

The work of Chew and G-B directly concerns the n-d reactions; we are interested in the mirror reaction so that when reading their work one must consistently read "proton" for "neutron" and "neutron" for "proton". Wherever their work is described in this thesis such a translation has been done. One thus assumes that the coulomb force plays a negligible part.

G-B assumed that only the singlet slow proton state was important (Z=0), and calculated the neutron energy spectrum due to charge exchange; their results at 0° , 10° and 30° are shown in Fig. 1. At any given angle they expect a very narrow neutron energy spectrum, about 1 MeV wide. As well as being of fundamental interest, such a narrow width would be useful in producing nearly monoenergetic high energy neutrons.

Other experimenters have looked at the fast nucleon emerging from this reaction (Hofmann and Strauch, 1953) or from the mirror reaction n-d (Powell: see Chew 1951), but due to a spread in beam energy of perhaps 20 Mev, and inadequate resolution in measuring the energy of the fast nucleon, it is hard to be sure that the two slow identical particles have less than 5 Mev relative energy. It will be seen later that unless one can be sure of this, one cannot be so sure of the presence of the Heisenberg force.

In contrast to the fast neutron spectrum, the proton pair energy spectrum will be easier to measure, even to a resolution of $\frac{1}{2}$ MeV, and it will scarcely be blurred by the present spread of less than 2 MeV in the beam energy. It should be noted that even a much larger spread in

beam energy, of say, 5 MeV, would not obscure the real structure of the pair energy spectrum, for although this is the mirror image of the fast neutron spectrum it always starts from the origin whatever the incident proton energy. Thus the pair energy distributions for different incident ent energies are expected to be almost identical, so that a spread in beam energy does not matter.

An obvious tool to measure the directions and energies of two particles from a reaction is the diffusion cloud chamber. A preliminary note describing this experiment has already appeared (Firth, 1959). However, before surveying the experimental part, there are two other reasons why this reaction is of interest.

It is not known whether three body forces are important among nucleons, and the simplest systems which one can study to find this out may be H³, He³ and the p-d, n-d reactions. The mathematical difficulties are considerable, but apparently not hopeless.

A better reason for studying this reaction concerns the nature of the n-n force. Since one cannot do n-n scattering experiments, one must rely either on properties of mirror nuclei or on n-d reactions, in order to make comparison with the p-p force. Chew and G-B did their calculations largely so that n-d experiments might be analysed to give information on the n-n force. Their three-body calculations may be inaccurate, however, and we are fortunate in having the p-d reaction to check their approximations more exactly by experiment. The present work does in fact suggest that their calculations are not sufficient.

By using a cloud chamber, one can get the maximum amount of information about this reaction, and this was the method employed. A diffusion cloud chamber working at 20 atmospheres was assembled, together with the necessary control equipment and gas handling system.

The supply of suitable deuterium for the chamber was a serious problem, due to the presence of excessive amounts of tritium in the deuterium generally available. Eventually some suitable heavy water was found, although preparation of the gas proved troublesome.

To analyse the cloud chamber stereophotographs, a rather unusual technique was developed, which consisted in the measurement of points directly on the film. The calculations to restore a point into three-dimensions, and to calculate the dynamics of an event, were elaborate, requiring the use of an electronic computer and a considerable amount of programming. Once the procedure is worked out, calculation of an event is very fast.

DEUTERIUM PREPARATION

It was mentioned earlier that it was not easy to get deuterium suitable for this experiment. For most uses, deuterium is available in commercial quantities at a low price. But since the era of hydrogen bomb tests, the heavy hydrogen extracted from ordinary water contains too large a fraction of tritium (about 10⁻¹²) to allow a diffusion chamber to work. This information was given by Dr. R. P. Shult of Brookhaven Laboratory. Apparently the weak beta activity provides more than enough ionisation to "de-supersaturate" the vapour in the chamber.

A Wilson cloud chamber would not offer this problem, and in fact a hybrid between the expansion and diffusion types has been built by W. Powell (1957) and used with "dirty" deuterium.

The largest fraction of tritium which can be allowed is said to be about 3 x 10^{-14} , which corresponds to 45 disintegrations per litre per second at 20 atmospheres. With the deuterium finally used one could actually see the very short β -ray tracks ejected by the tritium, and in one method of analysis for tritium (Fireman, 1954) one simply counts by eye the number of tracks seen in a small diffusion chamber.

The Oak Ridge Laboratory now supplies deuterium with a low enough tritium content for diffusion chambers, but at the beginning of the experiment it was not thought that this would be available soon enough, there being some question of priority.

But by an amazing stroke of luck, nearly a litre of heavy water was found in the laboratory. Although labelled simply 90% D₂0" its origin ensured its age being greater than that of hydrogen bombs or atomic piles. Of course if the water had been used as moderator in a pile it

would have absorbed enough neutrons to be quite useless for this experiment. Presumably at Oak Ridge special water, either from deep wells which have escaped contamination, or from glaciers or burnt petroleum, is used in the preparation of low tritium deuterium.

It was essential to extract all the deuterium from this heavy water, otherwise there would be scarcely enough to fill the diffusion chamber to 20 atmospheres. The obvious method of electrolysis proved unsuitable for just one litre of heavy water. For if one designs a cell large enough to electrolyse all the water in a few days, the volume has to be quite large no matter how one arranges electrodes and diaphragms. In that case there would not be enough water to fill the cell even at the start. Electrolysis seemed so obviously the most convenient method that a good deal of work was done in designing and building electrolytic cells which would require only a hundred c.c. or so to fill them. If one could allow the gases produced to mix, the problem would be much easier, but it seemed a poor idea to try to separate such a mixture.

In the end a chemical method was used, namely the reduction of heavy water by red hot magnesium. The apparatus for this comprised a reaction vessel heated in a furnace to 825°C, a means to inject known small amounts of heavy water into this vessel where the pressure was kept at about 50 p.s.i., and some pumping equipment to remove and store at high pressure the deuterium produced.

The pumping equipment was later used to handle the deuterium in the cloud chamber. Since no gas could be spared, a closed system had to be used, and tasks such as recirculation of alcohol in the cloud chamber had to be planned. The basic unit used in handling the gas was a hydraulic accumulator, such as is used in aircraft. This is simply a steel vessel divided into two parts by a rubber diaphragm, so

that by letting nitrogen at high pressure into one side of the chamber deuterium can be compressed into the other side. The arrangement of pipes, valves and gauges was rather complicated owing to the need for flexibility and is shown in Fig. 2.

There are two reservoir tanks because in pumping deuterium from below atmospheric pressure up to 900 p.s.i. the "dead spaces" in the system limit the compression ratio, and two stage pumping is necessary.

The reaction vessel was made of stainless steel and was heated to 825° C in the furnace. The reaction vessel is shown in Fig. 3a. There were three thermocouples arranged down the sides of the vessel because, as we shall see, the control of temperature was very critical. After much trial and error, the best gaskets were "home-made" from $\frac{1}{16}$ incopper sheet and annealed before use so that three sharp concentric ridges around the flanges at the end plate would provide a gas tight seal even at 850° C and 100 p.s.i.

The measuring device for the heavy water consisted of a thick walled glass tube whose ends were ground flat to seal against 0-rings in grooves in brass end plates. These end plates were pulled against the ends by brass caps which screwed onto an outer concentric brass tube. A longitudinal slit allowed one to see the level of water in the tube. Fig. 3b shows these components.

The procedure in an actual run was as follows:-

The reaction vessel was filled with dry magnesium turnings, the end plate and gasket clamped in position and the pipes were connected to the rest of the system, which then was pressure tested and afterwards evacuated. Heavy water was then introduced to fill the measuring tube, and the reaction vessel brought to a temperature of 625°C. The furnace was actually made of a cast iron pipe and had three separate heaters along its length so that a fairly uniform temperature could be kept.

The biggest problem during a run was to prevent the magnesium from melting. It melts at 650°C, whereas the reaction only goes with reasonable speed at 625°C or higher. Unfortunately the heat of reaction is considerable and only two c.c. of water can be introduced at a time or else the magnesium melts and reduces the area of metal which is exposed for the reaction. In fact, several runs were spoiled by this, but no heavy water was wasted.

In order to get high efficiency the apparatus was designed so that the entering gas (undecomposed heavy steam) met the lowest concentration of magnesium (i.e. partially oxidised magnesium turnings) whereas the gas passing through the last layers of completely unburnt magnesium contained only small amounts of heavy water.

The deuterium produced passed through a filter of glass wool which was kept at 0°C to condense any water vapour remaining. It also trapped magnesium oxide dust. The gas was then accumulated and pumped to a higher pressure in storage tanks.

Throughout the reaction the pressure was kept in the range 50 p.s.i. to 100 p.s.i. Since one molecule of deuterium is derived from one molecule of heavy steam and the other reactants are solid, the equilibrium is not affected by using high or low pressures. To inject the heavy water into the reaction vessel, a pressure of hydrogen was applied to the top of the heavy water column in the glass measuring tube.

Each complete run used 100 c.c. of heavy water, and as there were some runs which failed, the actual preparation lasted three weeks.

Much time was spent cleaning out solid slugs of magnesium from runs in which the temperature rose too high. Furthermore, since there was only

just enough deuterium for the experiment, excessive precautions had to be taken in all the work, to reduce the risk of losing any gas by leaks or catastrophes. So instead of being able simply to buy deuterium in a cylinder, the deuterium production took almost four months.

THE DIFFUSION CLOUD CHAMBER

Principle

The diffusion chamber was first suggested and built by Langsdorf (1939), but only came into serious use after the work of Cowan (1950) and of Needels and Mielsen (1950). The action of the chamber is rather different from that of the Wilson chamber, which uses the adiabatic expansion of a gas, saturated with a vapour, to produce cooling and hence a supersaturated gas. The diffusion chamber has a warm region where there is a supply of vapour, and a cold region where vapour condenses. The vapour pressure being higher in the warm region causes diffusion of vapour towards the cold region. If the temperature gradients are suitable, there is an intermediate region where the vapour pressure is higher than the saturation vapour pressure at the temperature of this region, Shutt (1951). In other words, supersaturation occurs because of extra vapour diffusing in, rather than because of a sudden cooling.

The advantages of a diffusion chamber are continuous sensitivity (provided the irradiation is not more than a few times normal background), and mechanical simplicity since there are no moving parts. Both these features are especially important at high pressures where a Wilson chamber has a very long recovery time. After intense pulses of radiation the diffusion chamber takes some time to become sensitive again, but far less time than a Wilson chamber.

Since one likes to use as high a density of gas as possible, to increase the number of interactions, these are important advantages and have led to the replacement of many Wilson chambers for use with accelerators and even with cosmic rays. (Since cosmic rays are mainly vertical and the sensitive layer is only two or three inches deep, the advantage

of continuous sensitivity is somewhat outweighed by the short length of path that can be seen.)

General references to the diffusion chamber may be found in the review by Slatis (1957).

Description of present chamber

In the present work a number of preliminary models of chambers were built and eventually one to work at five atmospheres. Several gases were tried, including sulphur hexafluoride which has a high stopping power and which worked fairly well. At this stage the idea of studying this particular reaction with deuterium arose, and it was obvious that a better diffusion chamber was needed to withstand the 20 atmospheres required. Fortunately, as a result of a visit to Brookhaven Laboratory, Dr. Shutt agreed to lend us an early model of chamber which they had used to get an understanding of the working of a diffusion chamber. This model was altered and used in this experiment. A section of the chamber is shown in Fig. 8.

The chamber is a cylindrical can with a window in the top and is divided around its middle by a bakelite insulating ring.

The bottom part has a $\frac{1}{4}$ in. bottom plate (2) and top flange (3), both made from cold rolled steel. At one side of the cylinder is a rectangular duct which ends in a face plate with an 0-ring groove against which is held a window.

The bakelite ring (5) separating the top and bottom parts is sealed by 0-rings against flanges welded to the top and bottom parts.

The bolts holding together top and bottom are thermally insulated from the top by bakelite sleeves and washers.

The top is a hat shape so that the window, being further from

the region to be photographed, may be made smaller. Also the vapour supply to the centre of the chamber is improved.

Construction of the two windows is similar. Two inch lucite provides physical strength but does not resist methanol used in the chamber, so it is backed by $\frac{1}{4}$ in. "Allite" sheet in contact with the 0-ring seals. A special 0-ring is used in the side window, since ordinary ones would harden with the cold and crack. Glass would be optically better than lucite but would crack more easily under non-uniform stress caused by temperature gradients in the chamber.

The top carries an alcohol reservoir in the form of a copper trough (9) making good thermal contact with the top. The sides of the top (11) are lined with felt which dips into the trough to get wet and increase the vapour supply.

A copper ring made of $\frac{1}{4}$ in. tubing hangs from teflon straps just below the window, but is large enough in diameter as not to impair the view. It is electrically connected to a Kovar glass lead through so that a sweeping field voltage may be applied to the chamber. About four inches from the bottom of the chamber several grounded wires are stretched across to shield the lower part of the chamber from the electric field and ensure that ions produced in the upper part of the chamber will not drift into the lower part.

On the bottom of the chamber outside are cooling coils (13). Copper tubes (14 and 15) carrying heating wires are soldered to the flange of the lower part and around three levels on the upper part of the chamber. These heaters allow one to vary the temperature of the vapour source and to vary the temperature gradient in the side walls.

Alterations

A number of changes were made to this basic chamber. According to Slatis and others, it is worthwhile to lower the temperature even a few degrees, so an extra cooling coil was placed <u>inside</u> the cloud chamber and soldered to a copper plate. Exit and entrance of coolant to the coil was through stainless steel fittings, extending through holes in the bottom of the chamber, and designed to use a minimum of vertical space in the chamber. These fittings had 0-ring grooves which sealed against the bottom of the chamber from the inside. In retrospect it is doubtful whether this extra cooling improved the chamber enough to be worth the amount of work and trouble involved.

During early runs it was noticed that there was a circulation of gas caused by the side windows, so that a dummy window was added at the inner end of the side port, and this stopped the circulation.

To help in taking apart and putting together the chamber - and this occurred often - a strong lifting framework could be bolted onto the top (which weighs sixty pounds and must be gingerly replaced).

The side walls of the chamber are $\frac{1}{4}$ in. thick stainless steel and would reduce the energy of 90 Mev protons to 60 Mev. So a cylindrical side arm five inches long and $1\frac{1}{2}$ in. diameter was welded into the wall, with its axis parallel to the side window and $1\frac{1}{2}$ in. above the new chamber floor. This side arm ended in a flange with an 0-ring groove sealing against a stainless steel cap with a curved portion 0.01 in. thick. This curved window was tested to 1200 p.s.i. pressure; although it was more work in design and machining than a flat window would have been, the loss in energy suffered by 90 Mev protons was only 1 Mev. The tubular side arm was filed smooth to allow

lead collimators to slide in, and several arrangements were tried.

Reflecting walls

During the earlier runs the inside walls of the chamber were covered with black velvet, as is the usual practice in cloud chamber work. However, there appeared to be no disadvantage in using a reflector around the inside of the cloud chamber, provided little light reflects or scatters from it into the camera. These conditions can be met if a fairly parallel beam of light enters the side window, and if one has good reflecting walls. Stainless steel resists corrosion, but has fine scratches along one direction and these badly scatter light incident in the plane perpendicular to the scratches. Light incident in the plane parallel to the scratches is not so badly scattered and a reflector cut properly was bent around the walls, increasing greatly the illumination without giving much glare into the camera lens. This addition allowed lens apertures of f/11 without overloading the flash tubes and also made illumination more uniform.

Temperatures of Chamber

To monitor the temperature of the chamber, eleven thermocouples were placed at various points and so connected that a twelfth common junction sat in melting ice and twelve copper leads ran to the control panel. They proved invaluable in finding and repeating the best working conditions for the chambers.

Leaks

Owing to the stringent need to conserve deuterium, only very small leaks could be tolerated, and the chamber in its original state was far from being tight enough. A large tank, four feet in diameter

and full of water was used to look for leaks with the chamber under 400 p.s.i. This method was very precise in locating leaks.

Several 0-ring seals leaked badly, so the flange surfaces were remachined where possible, or in the case of the side window hand filing and polishing was necessary. All soldered pipe connections were remade and in all cases new fittings were made.

There was some improvement, but the remaining leaks were mainly around the bakelite ring which was made of fibre based bakelite so that machining had left a rough cloth-like surface. The groove was enlarged, filled with epoxy resin and remachined. However, after a few weeks, the bond between resin and bakelite appeared to be weak in several places (as seen through the translucent resin), and it looked unsafe to rely on this ring. So a new ring was made from 1-in. paper base bakelite, and proved strong enough although at the end of the experiments the 0-ring groove edges were badly deformed under the pressure.

AUXILIARY EQUIPMENT

Cooler

Dry ice is the most convenient source of cold for a diffusion chamber, but it is not easy to keep the solid in contact with the chamber bottom except in simple models, so that usually a liquid cooled by dry ice is circulated through pipes on the bottom.

In this work alcohol was the coolant at first, but is inflammable and also viscous at dry ice temperature so that trichlorethylene (which is merely toxic) was used finally. A gear pump was used in the early circulating systems but was unsatisfactory as it would inexplicably seize up, perhaps due to small particles of dry ice. So eventually a turbine pump was bought and a new cooler built.

Because one can have neither lubrication nor an effective shaft packing at dry ice temperature using a liquid like trichlorethylene, the whole pump sat in a tub of trichlorethylene and dry ice. The pump hung on the end of a vertical shaft and housing of stainless steel, and was driven by a $\frac{1}{4}$ H.P. motor. A close fitting teflon bushing replaced the normal packing, so as to prevent too much leaking which, incidentally, did no harm as the liquid fell back into the tub. Glass wool wrapped in polythene bags (to keep out moisture) insulated the tub, and similar insulation was also used on the cloud chamber and on a storage bin for 100 lbs. of dry ice.

Heaters

Three heaters in series with each other and a variac and ammeter heat the top of the chamber; the main heater for the bottom of the chamber has a separate variac and ammeter. This arrangement was flexible enough to give the required top temperature at the same time giving the correct temperature gradient in the walls. The main heater took 8 amperes, the top heater 3.5 amperes.

Gas handling and alcohol recycling

After every run, most of the deuterium was pumped back into the storage cylinders by using an arrangement similar to that used for pumping in the production of deuterium. The leaking was negligible at a lowered pressure of 50 p.s.i.

In addition there was the need to remove alcohol which had condensed at the bottom of the chamber, and to restore it to a reservoir above the cloud chamber, so that during the run it could be fed by gravity into the trough in the top of the cloud chamber. This pumping of alcohol was a nuisance, so that by having two reservoirs, one to fill the trough, the other to drain the bottom, the operation need only be done every second run. The plumbing system to do this was complicated but not ingenious; no trouble occurred once all leaks were eliminated. No level indicators were used, and the recycling was followed by the gurgling sounds emitted.

Special mention must be made of the valves used throughout.

These were Hoke valves using an O-ring instead of the usual packing, and they do not leak with pressure applied from either side. At the start of this experiment they were a new product and they worked well obviating the need for packless valves at four times the price.

Lighting

A flash tube mounting and reflector came with the chamber, and provided the fairly parallel beam necessary when using reflectors around the chamber wall. The flash tubes were got with difficulty and seemed to be vastly overrated by the makers; they were driven by a bank of condensers (128 x 2 μ fd condensers) charged to 1500 v. by a high voltage supply designed to charge the condensers in three or four seconds. The condensers weighed 300 lbs and were built into a wooden box with shelves; it ran on casters and could conveniently be moved anywhere out of the way.

Photographic Background

In a Wilson chamber the dark background is usually black velvet, which is very suitable until heavily wetted when it scatters much light. The best background for a diffusion chamber is a pool of alcohol containing an alcohol soluble dye (for example nigrosine black, which is really dark purple). In this way one takes advantage of the unavoidable wet floor. This background was used in all preliminary experiments and

was excellent, but in the final experiment where the alcohol is to be recycled and the chamber cannot be opened, it was feared that the windows and walls would become darkened by the splashing from drops falling to the bottom. Black anodised aluminum was tried, but this is not very black even when wet, and the final solution was black glass; covered with a layer of alcohol this scatters very little light through the top window.

The black glass carried seven fiducial marks put at the centre and corners of a regular hexagon. These marks were small holes $\frac{1}{10}$ in. diameter drilled in the glass and filled with teflon. If they had been smaller one could still have seen them clearly on the photographs.

Camera

Most of the camera, including the lenses, was loaned with the cloud chamber. The lenses were 30 mm f/3 Bausch and Lomb movie lenses. The short focal length allows one to mount the lenses very close to the top window and about 30 cm. from the tracks to be photographed. With a chamber working at high pressure, one prefers as small a window as possible, and in that case the lenses must be near the window in order to see all the chamber. (Really, two very small windows, one for each lens, would be better, as much thinner windows could be used). To get the necessary depth of focus one must use a short focus lens.

The two lenses were mounted four inches apart, their optic axes making an angle of 17°. The lens mounting was separate from the film magazine with its advance mechanism. The lenses stay in position on the cloud chamber when the magazine is removed to reload. The lens mounting was fixed to a cap fitting closely onto a cylindrical can permanently attached to the cloud chamber. The camera could be re-

positioned to within $\frac{1}{20}$ in., although the method of measurement was insensitive to error in the exact position.

The film was unperforated linograph ortho, and with the increased illumination provided by the reflector inside the chamber, apertures of f/8 and f/11 were used.

The lenses were accurately focussed by trial and error, taking a photograph of an inclined sheet of graph paper inside the chamber, and shimming the lenses until the sharpest image was of an object 4 cm. from the chamber bottom.

Picture counter

In order to record a reference number on each photograph, a four digit telephone counter was modified by adding neon lamps to illuminate the numbers and by providing a time delay device to give the correct illumination. The device also increased the number each time the film was advanced.

Because the lenses were close to the window it was difficult to arrange to photograph the counter at the same time as the chamber. A kind of periscope was used made of two prisms with the counter mounted on a vertical tube attached to the lens plate and far enough away to be in focus. The tip of one prism was near the edge of one lens which was just able to see the prism "out of the corner of its eye".

A second counter was placed at the control panel and connected in series with this counter so that the two always kept in step.

Carriage

The equipment mentioned so far was all mounted on a rather light steel framework, with plywood floors and casters to allow movement up the corridor from the cyclotron room. Eventually rails were laid up the corridor and considerable remodeling was necessary to add wheels
to the framework and still to keep the correct height for the chamber.

(Some adjusting screws were added to the cloud chamber and certain height
saving changes made.)

Control equipment

The way of controlling the cloud chamber and cyclotron was changed several times to make it more reliable, and as experience was gained improved ways of running the system were found. The sequence of operations is as follows:-

- 1) The cyclotron is turned on for as many as twenty modulation cycles (afterwards called pulses) and protons pass through the cloud chamber.
- 2) A short period of waiting follows (10 to 300 milliseconds) to let the drops grow large enough to be visible.
 - The light is flashed.
- 4) The camera is rewound and the counter shifted, and an electric sweeping field of 1500 v. is now applied for up to two minutes, depending on the recovery time of the chamber.
 - 5) The sweeping field is removed and after a few more seconds.
 - the cycle is repeated.

Originally, time delays were set by univibrators, but the ones with long time constants (about two seconds) were unstable and easily triggered by spurious pulses from relays. The long time delay of two minutes was the most difficult to build, and even a thyratron in an R.C. circuit would trigger before it should. (The Miller effect was used to increase the effective size of a condenser and so get a long time constant.)

Eventually an electric clock timer was used for this long delay.

For shorter time delays up to a few seconds a reliable device was built to use the decay of current from an electrolytic condenser discharging through a sensitive D.C. relay and a series resistance. The current required to hold a relay down was about one quarter the current to pull it down. After the current has decreased enough, the relay opens. A Block Diagram of the circuits appears in Fig. 4.

Mechanism of firing flash tube

The flash tube was fired by discharging a small condenser charged to 150 v. through a thyratron and the primary of a spark coil; a high voltage pulse of about 10,000 v. from the secondary winding was applied to a spiral of wire wrapped around the outside of the flash tube which then discharged the large bank of condensers.

Other functions of the controls

This basic control system had several other uses. For looking into the chamber by eye a 0.5 μ fd condenser was charged to 1500 v. and discharged through the flash tube 50 times a second by applying the 10,000 v. trigger 50 times a second. This illumination is better than using a second source of light, since it allows one to see the chamber under exactly the same lighting geometry as used with the camera, so that one can correct immediately without developing film.

The clearing field could be applied continuously or switched off altogether. If a track is formed in a region with electric field a halo surrounds it, due to rapid spread of ions under the electric field.

The film could be advanced continuously, and the counters advanced independently.

Temperature measurement

A sensitive galvanometer stood on a special tray on the control chassis and could measure the e.m.f. of each of the eleven thermocouples simply by turning a 12 position switch. By using the correct series resistance, the meter was calibrated directly in degrees centigrade, and read from -70°C to +50°C.

Beam monitor

To monitor the beam, so that one could check its intensity and position, a thin crystal scintillation counter was mounted on the cloud chamber to intercept the beam which passed through the chamber. The amplified pulses were displayed on an oscilloscope at the cloud chamber controls. The experiment would have taken far longer without this monitor, which told if the beam was too intense or absent, so that the steering magnet current could be adjusted, or some fault discovered.

Temperature in a supersaturated region

It is of more than esoteric interest to discuss the measurement of temperature in a supersaturated region; in the literature on diffusion chambers no mention is made of this difficulty. Temperature is usually regarded as a property of equilibrium, whereas supersaturation is an unstable (or metastable) condition. But one must know the "temperature" at each point as well as the pressure in the chamber if one wants accurately to know the stopping power of the gas in order to find the energy of nuclear particles from their range.

If one tried to insert a thermometer or thermocouple in the sensitive region one would disturb the thermal conditions and also remove the supersaturation locally, so that the thermometer would no

longer be in a supersaturated region; furthermore this disturbance would be permanent.

In a similar way, the temperature of the side wall at a given height is not the same as the temperature of the supersaturated gas at that height. There is a region extending about an inch horizontally from the wall in which no tracks form, and presumably some convection takes place to maintain steady thermal conditions in the gas. From the practical aspect of repeating the best working conditions for the chamber, the temperature of the side wall may be just as good a parameter as the "temperature" of the gas, but it is not known by how much these two temperatures differ.

In principle at least, one might measure the density of the gas (and hence this "temperature"?) by finding the range of nuclear particles of known energy. However, in this experiment there was assumed to be a linear temperature gradient throughout the supersaturated region; the temperatures just above and just below this region could be measured directly with thermocouples.

COMBINED OPERATION OF CHAMBER, MAGNET, AND CYCLOTRON

The usual use of the Radiation Laboratory cyclotron for bombardments does not give rise to as many complications as a typical cloud
chamber run, during which three complex and unco-operative pieces of
equipment must work simultaneously. These are the cyclotron, the steering magnet, and the cloud chamber with its controls.

The procedure in an ideal and atypical run is as follows:

The pipe connecting the steering magnet and cyclotron had to be connected each time and well evacuated before opening the gate into the cyclotron, so it was best to pump overnight.

The cooling system for the chamber was switched on and loaded with fifty pounds of dry ice. A curious hesitancy occurred each time. (See footnote)

The chamber took about half an hour to come into proper working condition; then the heaters could be turned on, depending on the readings of the eleven thermocouples.

Re-alignment of the chamber was quite easy by using a string which had to cross fiducial marks on top of the chamber and align with marks on the walls of the corridor. (However, initial alignment was more complicated and was done by sighting along the tube through the shielding wall from both ends, using mirrors. X-ray films showed the path of the beam.)

Footnote: For about half a minute the coolant would circulate properly and the pressure gauge attached to the output of the pump would show 25 p.s.i. Then circulation would stop for two or three minutes after which circulation restarted quite suddenly. The effect was very likely due to the release of CO₂ which prevented the pump from working until everything was quite cold and the evolution of gas had lessened.

The cloud chamber was next filled with the gas, which was hydrogen or helium during practice runs but was eventually deuterium. Filling and emptying deuterium was a lengthy task, nevertheless to conserve the gas against small but ineradicable leaks, it was pumped back into the cylinders after every run. If necessary the alcohol for the lower reservoir was blown into the top reservoir, and the alcohol tray in the chamber filled to overflowing.

At each cooling and filling with gas the chamber gave forth ominous loud creaks and clicks, whose source was never traced but which never caused any harm. They arose most likely from the bakelite spacing ring or from the windows.

After the internal beam of the cyclotron was working properly, the thin scatterer was turned into position in the cyclotron, and the steering magnet and cooling water turned on. With the cyclotron running continuously, the steering magnet current was now varied until the external beam current through the cloud chamber was a maximum as measured by the crystal monitor. The cyclotron was then placed under the control of the cloud chamber controls, and a burst of protons allowed through every 90 seconds.

Owing to the small number of protons emerging, it was safe actually to watch the burst of protons pass through the chamber. As well as being a beautiful sight this was useful, for one could check the working of cloud chamber, monitor, steering magnet and cyclotron in this way. The appearance of the beam was the means of setting the best conditions of temperatures, pressure and recovery time for the chamber. Only with direct viewing can one rapidly know if conditions are wrong and so alter them. This is an advantage over the use of the Wilson

chamber in the cyclotron room.

The camera was next placed in position and all controls set to normal running position.

Due to the elaborate "setting up" required for the equipment it was best if a run lasted a full day, from 9.00.am until 10.00.pm.

By no means all of this time supplied photographs, although towards the end of the experiments about two-thirds of a day was useful running time.

Troubles with the steering magnet

These difficulties were many and have been dealt with more fully elsewhere (Radiation Laboratory Progress Reports, Firth and Hargrove).

The current regulator had many intermittent faults traced mainly to bad wiring and faulty components, but also there was some R.F. pick-up.

The steering magnet coil developed short circuits twice and a total of about six months were spent in connection with these break-downs.

The first breakdown was dealt with by adding a filling of epoxy resin at the flat ends of the coil where there were obvious short circuits. On replacing the coil a large number of leaks appeared along the whole of the external beam vacuum system. Eventually the vacuum box between the poles of the steering magnet was rebuilt. A useful temporary remedy proved to be a polythene diaphragm clamped between the pipe flanges across the pipe.

The second breakdown ended the series of experiments.

When the external beam was working once more (after the first breakdown had been repaired) a good deal of time was spent im-

proving the operation of the cloud chamber and preparing to run with deuterium. Several satisfactory runs were made with deuterium filling, but then the steering magnet again broke down and no more runs were made.

Troubles with the cyclotron

As well as the difficulties usual to the cyclotron are some which appear only during infrequent pulsing. On continuous run the cyclotron gives 400 pulses per sec. of more or less equal size. But if only one pulse per minute is used, the size varies enormously and very often no protons at all will arrive. Since there is an optimum size of burst for the chamber, such that one much larger obscures all events in the chamber and one much smaller provides fewer events, one prefers bursts of protons as uniform as possible.

At the start of the experiments, only one pulse each minute (of the 400 available per sec.) was taken, because the drops along the tracks were only allowed to grow for 10 millisec. before being photographed. However, when it was later found better to let the drops grow for 200 millisec., and therefore it was possible to allow twenty pulses in each burst, one expected that the uneveness in pulse size might be smoothed out. This was not so. An electronic integrator was built to measure the total number of protons in a burst.

This integrator satisfies somewhat different conditions from those usually met with in a "CR" integrating circuit. Here the signal to be integrated is a group of pulses each ten microseconds wide with 2500 microseconds between successive pulses. If one makes CR long compared with 2500 μ sec, very little voltage is induced on the condenser during the 10 μ sec duration of each pulse. So, if one makes

CR much smaller, and long compared only with 10 μ sec, the voltage induced is lost between pulses. Hence a diode must be incorporated to prevent this.

A germanium diode was used at first, but for the back voltages used (about 0.2 volt) the back resistance is only about one tenth of that for more commonly used voltages of 5 volts. An ordinary vacuum diode proved quite suitable.

The distribution of the sum of pulses in a burst was examined in this way and was found to be no more uniform than the distribution of a single pulse. In other words, if one pulse in a burst was small they were all likely to be small. Perhaps this is due to some variation of the ion source or in the ionisation of gas outside the ion source.

There is a second fault which occurs when one tries to pulse the cyclotron after a period of quiescence. The R.F. voltage often breaks down inside the cyclotron tank for about $\frac{1}{5}$ sec., so that at first no protons emerge at all. It seems as though ions accumulate somewhere when the beam is off, lie in wait to cause breakdown, but are swept away after about fifty modulation cycles.

Remedies for beam fluctuation

Naturally the various working conditions of the cyclotron such as voltages and pulse lengths were varied over a wide range, but to no useful effect.

Three remedies were designed and built, but only one was tried because the steering magnet broke down before the other two were completed.

The method actually tried was to keep the "frog" up and the

beam on for most of the minute before the cloud chamber was ready.

Then the beam was switched off, the frog lowered and the burst of protons sent through the chamber. A device was built to do this work and added to the control chassis; it performed well, but the bursts were not much more uniform in size. The frog takes too long to fall, so that quiescent conditions are restored.

The next remedy used the electronic integrator, which again measured the total beam passing through the chamber and when this total reached a certain value would turn off the cyclotron. But if the require time for a full burst was going to be longer than a predetermined time interval, the cyclotron was turned off before a full burst had accumulated in the integrator. This was to avoid too wide a range of drop growth which would otherwise occur.

The last remedy, suggested by Dr. Foster, was a mechanical shutter in the path of the external beam, with the beam running continuously. This device used a compressed air ram to drive the heavy steel shutter.

An electrostatic deflector was considered but seemed impractical here.

Slow fluctuation

As well as the large fluctuation from one burst to the next there was usually a slower variation over a period of fifteen minutes, which was dealt with by moving the scatterer in or out of the cyclotron tank. A movement inward of one millimeter almost doubled the intensity.

Troubles with the chamber and controls and improvements arising from runs with hydrogen and helium

<u>Leaks</u>: The reduction in size and number of leaks has been discussed earlier. Eventually the rate of leaking at 400 p.s.i. of

hydrogen was less than $\frac{1}{2}$ % per day; the temperature fluctuations of the room had to be taken into account in measuring this.

Fogging: When the chamber first ran with air at atmospheric pressure the top window fogged very badly. To warm the inside by heating the outside was difficult with a window of three inch lucite. A hot air gadget was built into the removable cover holding the lens plate so that hot air could be blown from a tube very close to the window directly between the lenses. It removed condensation, but also softened the lucite; a new window was made. Fortunately with light gases at high pressures fogging does not occur so easily.

During preliminary runs with hydrogen and helium several faults occurred, and these required dismantling of the chamber. This would have meant some loss of deuterium, had that been the filling, for not all the gas can be pumped back.

Insulation: The insulation to the sweeping field wire broke down under the alcoholic conditions in the chamber, so the wiring was replaced with teflon insulated wire. This does not allow alcohol so easily to form a film.

Quality of sensitive layer

The quality and depth of the sensitive layer were very poor at first. There were currents, turbulence, rain and many bare patches where tracks would not form.

The currents were reduced by adding a dummy window at the inside of the rectangular side duct. This window was draught proof at the sides, but not gas-tight, so as to allow the pressure to be the same on both sides. Also a thin aluminum foil covered the entrance to the beam tube.

Turbulence seemed due to wrong thermal gradients and too low gas pressure. Actually, at low pressures a diffusion chamber should be built for upward diffusion as the denser mixture of gas and vapour then occurs at the higher temperature.

Rain is believed to be due to ions produced in the upper part of the chamber. It is reduced by using a sweeping field. It also occurs in streamers if the temperature of the top is too high, the best results being found at 25°C.

The "holes" in the tracks were the most serious difficulty.

They are due to background radiation, so it seemed worthwhile to try

to reduce this by improving shielding and removing radioactive material

from the vicinity. There was some improvement, but the best remedy

was to have larger temperature gradients along the walls thereby, perhaps,
improving the ability of vapour to diffuse in and restore supersaturation.

About 7 C deg/cm gave the best results.

Some of these difficulties have been met with by other experimenters and the review article by Slatis deals with many of these problems and some others.

Collimation and beam intensity

It was important to have a very parallel beam of protons, since with high beam intensities the track of an individual incident proton could not always be distinguished. The number of protons scattered through small angles by collimation depends roughly on the ratio of thickness of collimator to size of aperture. Hence a very dense substance should be used, and here $\frac{3}{8}$ in. of lead was used.

Two horizontal slits were finally used, each $\frac{1}{4}$ in. high, $1\frac{1}{4}$ in. wide and placed six inches apart in the beam tube at the side of the chamber. Strictly speaking, these slits do not collimate the

beam, they merely produce the required cross sectional shape for a beam already quite parallel after being intercepted a long way from its source. The slit width was the largest allowed by the beam tube, and the $\frac{1}{4}$ in. vertical width was a compromise between a narrow slit giving a larger proportion of scattered protons, and a wider one giving protons at all heights in the sensitive depth. There is a larger chance that the reaction products from an event near the outside of the sensitive layer will not be seen to stop, thus making the event less useful.

By using low beam intensities, with about 50 protons per photograph, one can see how parallel the protons are. The mean square deviation was less than one degree.

The maximum useable number of protons was about 300 protons per photograph. This was estimated from the number of p-p scatterings (greater than a minimum value) with the chamber filled with hydrogen. It should be noted that the cross section for the number of events is half the "scattering cross section" for protons, since "event" implies two protons scattered, whereas "scattering cross section" for p-p scattering implies adding together the probabilities of either proton being scattered into a given solid angle.

Higher intensities can be used if the growth time for the tracks is decreased, but it then becomes difficult to tell if a slow proton track ends in the sensitive region or travels outside. Mostly the growth time was 0.12 sec., but at first times as short as 0.01 sec. were used.

Efficiency of collection of events

By efficiency we mean the number of useful events per hour of running time. It is difficult to choose the ideal conditions for

running, as will be seen from the following, which describes the connections and contradictions between various possible conditions.

In this experiment we must know the energy of one or both of the protons emitted, so that at least one track must be seen to stop in the sensitive region. For these reasons, a large sensitive depth and a high pressure (high stopping power) seem desirable. An intense pulse of protons repeated as often as possible will also give more events.

Unfortunately, a large sensitive depth and a high pressure tend to be incompatible and, still worse, a large sensitive depth is had only at the expense of quality. (Quality here means having few bare patches, uniform density of track throughout the sensitive layer and even speed of growth of a track.) In addition, the recovery time of the chamber is longer with a large sensitive depth, a high pressure and with large pulses of protons. Also, the ease of deciding whether a proton stopped depends very much on the quality of tracks, the length of growth time and the intensity of blackening of the film. But the blackening depends on the size of drops and the intensity of the proton pulse as well as the lighting.

In such a complicated situation, one can merely hope for a reasonable guess at the best conditions, and that after much trial and error. Only near the end of the series of runs were the better conditions achieved, and the series was cut short by the breakdown of the steering magnet. Due to the imminent breakdown (it was obviously due) time could not be spent measuring tracks, which is the real way to discover the amount of useful information contained in a run, and hence to choose the best conditions.

In this experiment, many more incident particles were used in each photograph than is usual with diffusion chambers. Commonly about fifteen or twenty mesons per picture have been used, and one can clearly see every track. With such an intensity the repetition time is about five seconds.

However, the ionisation per centimetre of a 90 Mev pion is only one-third of that of a 90 Mev proton, so to get the same ion load on the chamber would take only five protons. The ion load determines the recovery time, but not in a proportional way, for after extremely heavy doses of radiation (for example from a powerful γ -ray source) the chamber fully recovered in two minutes.

Thus it seemed preferable to use as many protons as possible per burst, provided the reaction could be seen, and to wait for the chamber to recover. The fact that we are looking for the relatively dense tracks of two slow protons helps us to see them amid the confusion of incident proton tracks.

With so many and such qualitative factors at play, it is hard to justify quantitatively those conditions which it seems best to strive for. However, it is better to aim at the following:-

- a) To sacrifice some sensitive depth by using warmer top temperatures (25°C) and larger temperature gradients (7 C deg/cm). The pressure may be 20 atmospheres.
- b) To use lower beam intensities, of about one hundred protons per photograph. Of course, the beam fluctuations make this difficult.

GEOMETRICAL MEASUREMENT OF TRACKS

The traditional way of measuring a track in a cloud chamber has been to take two photographs of the track with a stereocamera and then to reproject both pictures at the same time, using the original camera geometry.

Consider first the basic problem of finding the threedimensional position of a point. The reprojected images are located in three dimensions either by moving a pin until there is no parallax between its tip and both images of the point, or by moving a translucent screen until the two images of the point coincide. be emphasized that a sharp image of the point appears over a large distance in the direction of the lens. This is done by using small lens apertures in the reprojection, so that one does not have a sharp image at only one point. So the original point in three-dimensions, gave a point image on the film behind each lens, whereas reprojection of each point image produces a straight line in three-dimensions, and the intersection of the two straight lines reproduces the original point in three-dimensions. A track whose initial and end points are clearly seen may be regarded as two points in three-dimensions, and its length and orientation thereby found. Actually, with reprojection onto a translucent screen, one simply orients the screen and moves it back and forth until the two track images coincide on the screen, and the angles of the track may be easily read on protractors attached to the screen.

Reprojection has the advantage that the calculations are few and that corrections for the thick window of the cloud chamber are taken care of by reprojecting back through the window. Similarly.

thick lens corrections and even some lens distortions are compensated for. However, the film must be accurately replaced in the camera, and the whole method appears slower and intrinsically less accurate than one based on measurements of the images of the tracks directly on the film. In particular, if one has several fiducial marks whose images appear on each photograph, some corrections can be made (for example film shrinkage correction) which are impossible with a reprojection method.

In the present experiment neither the number of events nor the accuracy necessary really justify the length of time which was spent in developing a method of this sort. It is true there was one genuine factor which favoured this method of direct measurement on the film; the high beam intensity makes the two reprojected images together a confused mess, whereas separately it is much easier to sort out tracks due to reaction products. So this work on measurements is largely a quite separate project, which turned out to be very interesting and which could be further developed for future cloud chamber work.

The method used here was to treat each lens as a point, through which a ray from a point image on the film must pass, and to calculate the equations, in three-dimensions, of this ray in its passage from the camera, through the glass window and into the cloud chamber. The intersection of the two rays from the two images was calculated algebraically yielding the co-ordinates of the original point in three-dimensions. Obviously if the two calculated rays truly correspond to the original light rays they must intersect, and this fact was used in the following way.

A quantity called Δ (see Appendix A) measures how closely the two rays approach each other, and hence measures the inaccuracy

of the measurement. Consider, however, the problem of finding the direction in three-dimensions of a line whose end points are not known. One wishes to choose two points on this line, photograph them and from the images to calculate the original two points in three-dimensions. But there is no way of recognising corresponding points on the two photographs of the straight track.

To fix our ideas, let the co-ordinate system in three-dimensions be defined in the camera geometry by taking the X-axis parallel to the line joining the points representing the two lenses. The Z-axis is then so chosen that the X-Z plane is perpendicular to both film planes. On each film plane choose x-y axes such that both y-axes are parallel to the Y-axis.

Let the original track, which need not be a straight line, be given by:

$$X = X(s),$$
 $Y = Y(s),$ $Z = Z(s)$ (1)

where s is a function of the distance along the track. Then, if the two-dimensional curves on the film are given by

$$f_1(x_1y_1) = 0$$
 $f_2(x_2y_2) = 0$ (2)

(Subscript 1 applies to the left lens, 2 to the right) we work as follows:

X, Y, Z and Δ are each functions of (x_1, y_1, x_2, y_2) and the camera constants, so choose a pair (x_1, y_1) and (x_2, y_2) which lie on their two-dimensional line images, and calculate the quantity Δ , which measures the closest distance of approach of the two rays (one from (x_1, y_1) , the other from (x_2, y_2)). Then, keeping (x_1, y_1) fixed, keep choosing pairs of (x_2, y_2) satisfying $f_2(x_2, y_2)$, i.e. lying on the two-dimensional curve image, until Δ becomes zero. From the four final values (x_1, y_1, x_2, y_2) giving $\Delta = 0$ then calculate (X, Y, Z), thus getting

one point on the curve of equation (1). Other points on the curve in three-dimensions are then found by taking a different (x_1, y_1) and repeating this calculation.

From a practical point of view two difficulties emerge; firstly the enormous amount of calculation, and secondly the need that Δ should be a sensitive test for the correspondence between (x_1, y_1) and (x_2, y_2) . The first problem can only be solved by using an electronic computer, but this was necessary anyway in fitting the camera constants to known fiducial marks. The second problem can be solved in all cases by using three cameras instead of two, and arranged preferably in an isosceles triangle, but at least not in a straight line. Then one has three Δ^t s instead of one, and at least one will be sensitive. Unfortunately, only two cameras were used, and since errors in measurement can also contribute to Δ , tracks having some orientations were not measured as well as one would like.

It is obvious that the method used here (see Appendix A) is algebraically complicated, and it is interesting to see if there are simpler methods. One can find approximate formula which are nevertheless very accurate, and involve simple functions of the (x_1, y_1, x_2, y_2) such as $x_1 - x_2$, $x_1 + x_2$, x_1x_2 . Alternatively, by the use of a great many fiducial marks throughout the whole chamber, it might be possible virtually to eliminate corrections due to the thick window.

Another and completely different approach might be to use the fact that a straight line in three-dimensions is transformed into two straight lines in two-dimensions; this is apparent from the proton tracks. Although this means we have some sort of linear projection, it is not true that X, Y and Y are linear functions of (x_1, y_1, x_2, y_2) .

It seemed more direct to use a detailed analysis of the path of the rays; it might be best to get an approximate formula from this work.

The computer at the University of Montreal was used for all these calculations. It is a Royal McBee LGP-30 working on a binary basis, and is quite simple to learn to use and to write programs for. A total of five months were spent on the calculations, but much of this was occupied with learning various approaches to computation.

Broadly speaking, there are two ways of using the computer, called "fixed point" and "floating point". "Floating point" working takes account of the binary point of every number, so that in writing a program one need not consider the size of each number; the machine In "fixed point" working all numbers are reduced to numbe rs less than unity and the reduction is not remembered by the machine, so one must keep track of it in writing the program. Furthermore, one must arrange that a number is never divided by a smaller one, as this would give a number larger than unity (assuming positive numbers). With the LGP-30, floating point working takes about twenty times as long as fixed point working, so all programs were finally written in fixed Two factors were useful in arranging that numbers in the machine stay below unity. Firstly, the final results such as coordinates (X Y Z) lie within the known bounds of the chamber, and secondly one can with great advantage use direction cosines which must be less than unity.

For all problems met in this work in three-dimensions the three direction cosines are far more useful than a pair of angles in defining a direction. With a computer there is still another virtue;

to work out a cosine of an angle takes about 100 times as long as to multiply two numbers. Using direction cosines consistently, the most complicated function is an occasional square root.

We shall describe the calculation of lengths and directions of tracks by discussing the three programsthat were finally used to do this.

The "main program" requires two pairs of film measurements (x_1, y_1) and (x_2, y_2) , and the constants of the camera

$$f_1$$
, f_2 , A, n^2 -1, t, , β_1 , β_2 , S

(see Appendix A); it will calculate X, Y, Z and Δ of the point according to formulae in Appendix A. The other two programs both use the main program as well.

The "optimising program" was designed to choose values of six of the camera constants so that calculated positions of the fiducial marks gave the best fit to their known positions. This "optimising" was necessary because not all camera constants could be accurately measured.

The "event program" calculates a complete event, even if the origin of the event cannot be seen, and if neither proton stops. The results for each proton appear as a length and three direction cosines relative to the incident proton direction. Other quantities are also given, such as the co-ordinates of the beginning and end of the tracks, and all relevant $\Delta^{\dagger}s$.

Main Program

The reconstruction of a point as the intersection of two rays, one from each lens, was greatly complicated by the thick window. The

origin for the (X Y Z) was the central fiducial mark, and for the (x_1, y_1) and (x_2, y_2) it was the image of this mark; the orientations of the co-ordinate systems have already been described. It would have simplified the formulae if this origin had coincided with a "natural" origin formed by the intersection of two rays, one through each lens and perpendicular to each film plane. Given the formulae in Appendix A, there is no great difficulty in calculating the $(X Y Z \text{ and } \Delta)$ apart from keeping all numbers less than unity.

Optimising Program

The fiducial marks consisted of six points at the corners of a regular hexagon, with the centre mark of the hexagon acting as origins in the chamber and photographs. There are many possible criteria of goodness of fit, a natural one being that if \underline{r}_t is the true position of a point and \underline{r}_c the calculated position, then $\sum (\underline{r}_c - \underline{r}_t)^2$ should be a minimum. The sum is over all fiducial points.

But in this case we do not know the <u>r</u>_t because the orientation of the hexagon, relative to the axes defined by the camera, was not known. One can calculate the best orientation, and hence the most likely <u>r</u>_t and then proceed as above. The formulae for this were developed, but they were quite complicated, and also involved the use of inverse trigonometric functions, whose calculation on the LGP-30 takes a relatively long time. So it is better to use criteria involving only the relative positions of the six points with respect to each other and to the centre.

If $\underline{r}_{\underline{i}}$ is the calculated position of the i'th corner, and R is the real radius of the hexagon, then $(\underline{r}_{\underline{i}}^2 - R^2)^2$ and $[(\underline{r}_{\underline{i}} - \underline{r}_{\underline{i}+1})^2 - R^2]^2$

should be minima. These conditions require the hexagon to be regular and plane and errors, within the plane, in the calculated positions will easily be reduced by minimising the sum of these two quantities (called \mathbb{F}_1^2). But errors perpendicular to the plane hardly contribute to these expressions so these errors must be reduced some other way.

Apparently $\underline{r}_i + \underline{r}_{i+3}$ should be zero if \underline{r}_i and \underline{r}_{i+3} are exact, and hence we can minimise $\sum (\underline{r}_i + \underline{r}_{i+3})^2$ called F_2^2 . This criterion somewhat limits the possible errors perpendicular to the plane of the hexagon, although there is a relatively weak restriction on buckling around the hexagon. (Buckling here means say, odd corners up, even corners down; see Appendix A for better criteria).

A suitable mixture of F_1^2 and F_2^2 was used as the optimising criterion. Errors in calculated \underline{r}_1 affect F_1^2 much more than F_2^2 because the \underline{r}_1 are squared before subtracting R^2 . Hence F_2^2 was multiplied by a suitable factor so as to give all errors roughly equal weight.

 ${\rm F_1}^2$ and ${\rm F_2}^2$ should approach zero as the correct camera constants are found, and so also should $\Delta_{\rm i}^2$. In fact all these three quantities did decrease together when the chamber constants were varied to minimise ${\rm F_1}^2 + {\rm F_2}^2$. This suggests that the chamber constants and the formulae had some truth; one can fit a "best curve" to any set of data, but it is more meaningful to fit the right kind of curve.

The six camera constants (let θ_1 represent one of them) were fitted by calculating $F^2 = F_1^2 + F_2^2$ for a certain value of θ_1 , then increasing θ_1 by $\delta\theta_1$ and recalculating F^2 . If $F^2(\theta_1 + \delta\theta_1) - F^2(\theta_1)$ is negative, again increase $\theta_1 + \delta\theta_1$ by $\delta\theta_1$ and so on until

$$F^2(\theta_1 + n\delta\theta_1) - F^2(\theta_1 + \overline{n-1} \delta\theta_1)$$

becomes positive. At this stage the size and sign of $\delta\theta$ are changed by multiplying by $-\frac{1}{2}$ and the calculation recrosses the minimum in smaller steps $(\frac{1}{2}\delta\theta_1)$. After a chosen number of reversals this process is stopped, and another of the variables, say θ_2 , is selected and F^2 minimised with respect to it. In this way all six variables θ are varied after which the whole process is started again with θ_1 , and so on.

A diagram of the program is shown in Fig. 5; it was made quite versatile so that one could very easily change the variables θ , and the quantity to be minimised. The size of the increment $\delta\theta$, the reversal factor $(-\frac{1}{2} \text{ here})$, the number of reversals of $\delta\theta$ and the number of traversals of the whole cycle of variables, could all be easily varied. The camera constant θ_i after being varied must every time be replaced in its correct position in the main program.

The variables were optimised for fifteen hours by the computer and the variable θ was exchanged about 500 times. The points were fitted to a mean accuracy within the plane of the hexagon of 0.02 cm.; mean vertical accuracy was 0.05 cm.

Event Program

For each nuclear event found, measurements (x, y) on each film were made of the following points in the chamber and on the proton tracks:-

- 1) The image of the central fiducial mark.
- 2) A point on each track as near as possible to the origin of the event.
- 3) A point on each track either at the end if it stopped, or as near the apparent end as possible if it did not stop in the sensitive region.

These numbers total twenty and each was a five figure number, as read on the comparator.

Figure 6 shows the scheme of this program. The numbers are first related to their origin, which is the fiducial image. It is simpler to do this subtraction in the computer and also more reliable. Next the (x_1, y_1) left, and (x_2, y_2) right, referring to the intersection of the line images of the two tracks, are found and this point in three-dimensions is calculated.

Then the end points of each track (A and B) are found by fixing one point, say (x_1, y_1) on the left picture of track A and varying (x_2, y_2) along track A on the right picture, until the quantity Δ reaches a minimum; the (X Y Z) are then calculated with these minimising (x_1, y_1, x_2, y_2) .

There is a serious complication in this, because the computer must have numbers bounded within a certain region, and if the equation of the image of a track is used in the form y = mx + c, m can be very large. So one must test for this possibility, and if m > 1 then y is used as the independent variable and $x = \frac{y-c}{m}$. In addition, depending on the quality of the pictures it is sometimes better to fix the point on the right picture and vary the point on the left, so that provision must be made to do this according to code numbers which were fed in with the twenty co-ordinates mentioned earlier.

So far this "event program" has calculated the co-ordinates of the origin of the event, and the two end- or quasi- end points. This information was printed, but one really wants the lengths and orientations of the tracks. As the (X Y Z) are already in the memory of the machine one might as well add a small program to do this. The direction cosines relative to the co-ordinate system of the camera are

easily formed from

$$\frac{x - x_0}{\left[(x - x_0)^2 + (y - y_0)^2 + (z - z_0)^2 \right]^{\frac{1}{2}}}$$

but if the direction cosines of the incident proton beam are supplied, one can rotate into another co-ordinate system so as to calculate the two slow proton tracks relative to the incident proton direction. This information is then printed.

The geometrical part of the calculation is finished at this stage and one must now calculate the energy of the proton from its range, knowing the density of the gas, by using range energy tables. This part was done by hand, although it is not hard to add an interpolation program to do this with the computer.

The time to calculate one complete event was about seven minutes. With a small modification, a calculation could be done without minimising Δ^2 , and this took 100 seconds; printing the results took most of this time.

Accuracy of measurement

By measuring glass filaments of known length, the vertical accuracy was found to be about 3%. For distances nearer the horizontal, the error was considerably less than this, approaching 1%. Although this accuracy may be as good as necessary for this experiment it is interesting to consider the causes, and ways of reducing the error.

The comparator can be read to one micron, but cannot be set on the fiducial marks to better than 20 microns. However, if this is the only error in the (x, y) co-ordinates which are mostly of size 1 cm, it is not too large.

All calculations are done to a decimal equivalent of nine figures and little error enters from this source.

The biggest errors seem due to the minimising of Δ^2 to locate corresponding points on the two pictures. If the Y co-ordinate varies only slowly as we move along the track, Δ^2 is not so sensitive to error in the location of (x, y). Also, even if the correct corresponding co-ordinates (x_1, y_1) and (x_2, y_2) are used, Δ is never quite zero, so the requirement that it should be will actually select a pair (x_2, y_2) which does not quite correspond to (x_1, y_1) . Thus the source of error which makes Δ different from zero, even for corresponding points, must be found. It is thought that errors in the camera constants and errors in the (x, y) measurements are the main cause.

There is one type of error in the (x y) values which can be Translational errors in the position of the film either in removed. the camera or the comparator do not matter, since all measurements are referred to the image of the central fiducial mark. However, there seems sometimes to be a small rotation of the film as it goes across one of the film planes in the camera, whereas in the comparator the edge of the film is taken as the direction of the x-axis. The rotation was measured in a few cases and was less than $\frac{1}{2}$; if necessary one could accurately allow for it in the measurements, by measuring several fiducial marks and finding the rotation necessary to bring the marks into a standard position (this position would be found in the optimising An approximate allowance was made by minimising the quantity $(\Delta - \Delta_0)^2$ instead of Δ^2 . Δ_0 is Δ for the origin of the event. only a few cases did this produce a large change in the results. Tracks nearly parallel to the X-axis were the least accurately measured, owing to insensitivity of Δ^2 in correlating a point on the left picture with its corresponding point on the right picture.

KINEMATICS OF AN EVENT

To compare experiment with theory we need to know the direction and energy of the fast neutron produced in the reaction.

Also the vector momentum \mathbf{p}^t of the two slow protons relative to each other may give a deal of information, especially as to whether or not these protons are in an $\ell=0$ state. These quantities, and others simply related, were calculated with the computer.

We shall first discuss the least amount of information needed to solve completely the kinematics of this event. We assume that the momentum \underline{p}_0 of this incident proton is fully known.

Each of the three nucleons has three momentum components making a total of nine unknowns. But we know the direction of both slow protons from cloud chamber photographs; these directions give four known quantities. Conservation of momentum and energy supply four equations so that apparently only 9 - (4 + 4) or one extra quantity need be known. This is the momentum of one of the slow protons, deduced from its range in the gas; if both protons are seen to stop in the sensitive region, the event is overdetermined and one can check the accuracy.

Thus there are three possible states of knowledge of an event:
Overdetermined, with both proton energies known, fully-determined,
when only one energy is known, and under-determined, when neither energy
is known.

Later we shall discuss the "indeterminacy" due to errors in measurement, but there is one basic ambiguity which, it must be admitted, was only discovered in the later stages of the calculation.

From Appendix B, the equation to determine an unknown slow proton momentum x_1 when x_2 is known is:

$$x_1^2 + x_2^2 = \lambda_1 x_1 + \lambda_2 x_2 - x_1 x_2 \cos \alpha - k^2$$

where momenta relative to the incident momentum are used, e.g. $x_1 = \frac{p_1}{p_0}$.

There are two roots for

$$x_1 = \frac{1}{2} (\lambda_1 - x_2 \cos \alpha \pm \sqrt{(\lambda_1 - x_2 \cos \alpha)^2 + 4(\lambda_2 x_2 - x_2^2 - k^2)})$$

and by examining limiting cases, and a few actual examples, it appeared that one must take the positive square root in all cases. In many examples one root of the equation is negative, implying that the momentum should be reversed, but since the photographs show otherwise one can indeed rule out such solutions.

Unfortunately, for a certain range of λ_1 , λ_2 , x_2 , $\cos \alpha$, both roots are positive; in fact if

$$\lambda_1 > x_2 \cos \alpha$$
and $k^2 + x_2^2 > \lambda_2 x_2$.

One might hope to decide in some cases which positive solution is the correct one, if the two solutions differ widely. For example, from the density of the track it ought to be obvious whether the proton had 30 MeV or only 3 MeV. Also the minimum energy of a proton is known from the length of the visible track made before it left the sensitive region, and if this is much larger than the energy implied by one of the roots, one can reject that root.

However, we have to deal with experimentally determined quantities which may, in some cases, be so unhappily related (even if not simply wrong) that the ambiguity cannot be resolved with enough certainty. The confidence placed in the calculated values of x₁ will

be discussed later.

Only overdetermined and fully determined events were analysed, and both roots were used in calculation, for comparison. Also the overdetermined events were calculated (without using the quadratic relation) by using both proton momenta x_1 and x_2 directly from their range.

According to Appendix B, the angle \emptyset which the neutron makes with the incident direction is:

$$\cos \emptyset = \frac{1 - (\lambda_1 x_1 + \lambda_2 x_2)}{\left[1 - (x_1^2 + x_2^2 + 2k^2)\right]^{\frac{1}{2}/2}}$$

and the energy of the proton pair is simply $p_1^2 + p_2^2$ or $p_0^2(x_1^2 + x_2^2)$.

The relative momentum in the centre of mass of the two protons must be related not to a frame of reference given by the incident proton direction and some arbitrary azimuth, but to the scattering frame. One could choose as axes the incident direction and the direction perpendicular to the plane of the incident proton and the scattered neutron. Actually the frame of reference chosen had its Z-direction perpendicular to the plane of \underline{p}_0 and \underline{p}_0 , where \underline{p} is the sum of the momenta of the two slow protons, and its Y-direction in the direction of \underline{p}_0 .

One may regard the transformation in two parts, of which one is simply a Galilean transformation into the centre of mass, with all directions still measured relative to the laboratory system; the second part is then a rotation into the scattering frame. The rotation changes from event to event, (since P changes) which complicates the calculation.

Despite the importance of calculating in the centre of mass scattering frame there is some interest in knowing the various directions relative to the laboratory, since the cloud chamber measurements are almost certainly not isotropic in detection. In principle, using

polarised beams, such knowledge would also be fundamentally interesting.

The computer program to do this work was called the "kinematic" program; it was quite simple and rapid to write. For each event, the data supplied were the directions of the two slow protons, and the energy of one or both of the protons. The quantities calculated and printed included x_1 , x_2 , $x_1^2 + x_2^2$, $(p_1^2 + p_2^2)$ in Mev, $x_1(\text{calc.}) - x_1(\text{min.})$, and $\cos \beta$, as well as the original direction cosines of the two protons. The printed results of the centre of mass calculation were the total energy in Mev in the C.M., the direction cosines of the momentum in the C.M. of the two slow protons but relative to the laboratory axes, and also the direction cosines relative to the scattering frame.

These calculations were very rapid, total calculating time being about five seconds for a whole event, including the centre of mass transformations. However, each event used a full minute, because input and output of the data are slow, and many results were printed.

By hand these calculations would be very tedious, whereas writing a program is faster and a more interesting exercise than arithmetic. Also, there is another advantage in that the calculation may be altered by a very simple addition to the program (for example to use the negative square root instead of the positive one) whereas by hand, this takes almost as much labour as for the original calculation.

RESULTS AND DISCUSSION

Results

About four thousand photographs were taken of tracks in the chamber filled with deuterium. More than half of these had to be rejected owing to excessive intensity of beam or poor conditions in the chamber. The film was scanned by using a projection screen attached to a comparator; this was a boon, especially since the measurements could be made with the same arrangement as used for scanning.

Altogether 101 events were found with two dense tracks, and these are believed to be examples of charge exchange. Of these 101 events, in only 18 cases were the end points of both tracks seen; in 16 cases neither end point was seen, but the density of the tracks made it almost certain that both protons had low energy. The remaining 67 events, with just one track stopped, formed the bulk of the data, whilst the 18 overdetermined events provided a check on the method of analysis.

One might expect these 18 events, being the best known, to provide the most reliable distributions, were it not for two factors. Firstly, with 18 events the statistical errors will be large, and secondly, the probability of finding both protons stopped is greater for a lower energy pair, so that the use of only overdetermined events would bias the distributions in favour of lower energy proton pairs.

The second argument could certainly be applied to the 67 fully determined events, but as there are only 16 underdetermined events, one would expect the alteration in the results caused by the inclusion of these 16 (were they fully known) to be relatively small. The 16 underdetermined events were not used, except in this manner of

establishing that the results are not too biassed by selection at this stage. They could be used, with the other results, to find the distribution of the angle between the protons, which is related to the width of the energy spectrum.

As well as events with two slow protons emerging, there were inelastic events with one very fast proton emerging, and also some elastic scatterings. About one in six, out of all events, had two slow protons, but no attempt was made to measure absolute cross sections; this could perhaps be done by using the number of p-p collisions with the 10% of hydrogen in the deuterium.

As described in the last chapter, several quantities for each event were calculated and after further selection the results were drawn up in the form of histograms. This selection arose in deciding whether to take the positive or negative square root in the expression for x_1 in terms of x_2 , λ_1 , λ_2 and $\cos \alpha$. In a few cases it was not possible objectively to decide, and so rather than guess or favour one solution with an eye on G-Bis theory, these events were rejected, even though the total number of events is already rather small.

One would like to know the distribution in energy and angle of the neutron emitted, but with the number of events available, it is impossible to classify in terms of two quantities at the same time. The number of events in a "bin" selected for both energy and angle would be only one or two.

In all histograms, the shaded areas represent overdetermined events; the remainder of the events are fully determined.

Angular distribution of fast neutrons

Histogram 3 shows the distribution of $\int \frac{dn}{d\theta dE}$ dE, that is, of neutrons with angle irrespective of their energy. All azimuthal

angles are included, and this is equivalent to taking $\int \frac{d\mathbf{n}}{d\Omega d\mathbf{E}} \sin \theta \, d\mathbf{E}$; where θ is the angle between the neutron and the incident proton direction. The histogram is plotted with $\lambda = \cos \theta$ as abscissa, instead of θ . (If the differential cross section $\frac{d\sigma}{d\Omega}$ is given as a function of θ , it is most easily integrated numerically over Ω , by plotting as a function of λ and integrating with respect to λ . Since $d\lambda = \sin \theta \, d\theta$ the integration over azimuth is thereby included.)

For events in which both protons stop, so that x_1 and x_2 are known directly from experiment, it is interesting that $\lambda = \cos \emptyset$ may be expressed in terms of invariants. That is to say, we need not know the directions of the co-ordinate axes, nor of the incident proton relative to these axes. In Appendix B we have:

$$x_1^2 + x_2^2 + k^2 + x_1 x_2 \cos \alpha = \lambda_1 x_1 + \lambda_2 x_2$$

and substituting into the expression for λ gives:

$$\lambda = \frac{1 - (x_1^2 + x_2^2 + k^2 + \underline{x_1} \cdot \underline{x_2})}{\left[1 - (x_1^2 + x_2^2 + 2k^2)\right]^{1/2}}$$

Thus λ or \cos Ø is not so dependent on some of the errors as are other quantities.

Neutron energy distribution

It is of interest to know whether the neutron energy spectrum at a given angle is as sharp as the prediction of G-B says. Since the minimum energy of the neutron depends on its angle (from simple kinematics) the narrowness of the spectrum will be obscured on integrating over all angles of the neutron. This effect is not altered by looking at the proton pair energy, and histogram 2 shows the distribution of proton pair energies without regard to the angle of the neutron. In

other words, this is essentially $\int \frac{\mathrm{d}n}{\mathrm{d}E\mathrm{d}\Omega}\,\mathrm{d}\Omega$. This distribution is quite broad, and its most likely maximum occurs at about 7 Mev. As explained earlier, however, this does not mean that at a given angle the neutron spectrum will be as broad as this spectrum. This distribution could be compared with theory by evaluating $\int \frac{\mathrm{d}\sigma}{\mathrm{d}E\mathrm{d}\Omega}\,\mathrm{d}\Omega$ as a function of energy, using the predicted values of G-B. However, there is a device by which such a complication is made unnecessary.

From kinematics it is apparent that at a given angle the neutron has its maximum energy when the two protons have the same momentum, $\underline{p}_1 = \underline{p}_2$. In other words, when the energy of the two protons in their centre of mass is zero. In Appendix C it is shown that the energy distribution of the protons in their centre of mass (even though all neutron angles are included together) closely represents the shape of the neutron energy spectrum at any single angle. This is true provided the shape of the neutron energy spectrum does not vary much with angle, although the position of the maximum energy and the amplitude obviously do vary with angle. Thus, if we use the centre of mass energy of the proton pair, we need not distinguish neutron angles, and in this way we need not classify the events in terms of two variables at the same time, so that statistical errors are improved.

According to Appendix 3, the spectrum of centre of mass energies irrespective of neutron angle will have very nearly the same shape as the spectrum of neutron energies at a fixed angle. In particular, a width ΔE in the neutron energy spectrum will give rise to a width ΔE in the pair centre of mass energy spectrum. These considerations are true whatever angular distribution the two protons may have in their centre of mass.

The energy in the centre of mass is $\frac{1}{2} (p_1^2 + p_2^2 - 2p_1 \cdot p_2)$ so that once again we have a quantity which is independent of any knowledge of the beam direction, provided x_1 , x_2 and $\cos \alpha$ are known. (The proton pair energy in the laboratory system, $p_1^2 + p_2^2$ is obviously a similar quantity).

Histogram 1 shows the distribution of centre of mass pair energy. For the overdetermined events, the width at half maximum is about 2 Mev, and all events together have a half width of about 4.5 Mev. These widths imply neutron energy spectrum widths of 2 Mev and 4.5 Mev respectively. The curve on histogram 1 shows the energy spectrum according to G-B.

Angular distributions in C.M.

The angular distribution of protons in their centre of mass might be expected to tell whether the two protons are relatively in an S-state, or a P-state, or some mixture. It seems likely if the angles are measured relative to the scattering frame that any anisotropy will show, provided the measurements and transformations are sufficiently accurate.

Histograms 4, 5 and 6 show the angular distributions of the slow protons relative to the three axes defined in the slow proton centre of mass scattering frame. There is apparently anisotropy in the distribution of λ^{1} , both for overdetermined and for fully determined events. (Strict isotropy with direction cosine as abscissa yields a horizontal line.)

Discussion

The results will be discussed by starting with the most certain and progressing to the more speculative.

It is evident that many proton pairs are produced with energies below 10 Mev, showing that about 80 Mev of energy can be transferred from the incident proton to the neutron in the deteron. We explain this by charge exchange forces.

About one-third of the proton pairs have a relative energy below 2 MeV, indicating that the two protons are relatively in an $\ell = 0$ state, and hence have spins antiparallel. Since the two slow protons are in a singlet state, whereas the two nucleons in the deuteron were in a triplet state, we conclude that the exchange of charge can occur with spin flip.

It is interesting and may be apposite, to notice that in a favoured meson theory of nuclear forces, charged mesons are emitted from the nucleon source into states with $\ell = 1$. Exchange of such a charged meson between a neutron and a proton would exchange the charge and flip the spin.

Although a third of the proton pairs have C.M. energy below 2 Mev, at least another third have energy above 5 Mev, in contradiction to G-B who estimate that half the proton pairs should have relative energy below 1 Mev. Inclusion of underdetermined events would be likely to increase somewhat the proportion of higher energy pairs, thus making the discrepancy greater.

The angular distribution of fast neutrons varies rapidly with their angles, roughly as predicted by Chew and G-B. However, a histogram was calculated using G-Bts theory and is drawn in dotted line on the histogram 3. According to Chew, a triplet state contribution will decrease the proportion of neutrons emerging at small angles, and for the group with λ between 1 and 0.95 the observed number of events

falls somewhat below the G-B prediction, suggesting that the triplet state contributes to the reaction.

The histogram 4 for the distribution of λ^{ℓ} shows some anisotropy, which might be due to a combination of $\ell=0$ and $\ell=1$ states, although it is hard to see why the maximum should occur at about $\lambda^{\ell}=\frac{1}{2}$. Perhaps with an accurate C.M. angular distribution one could tell whether the state is a mixture of $\ell=0$ and $\ell=1$ states, but the present data are not sufficient.

We shall now mention an alternative explanation of the apparent charge exchange, and discuss reasons why the energy spectrum is wider than expected.

One can easily imagine a "head-on" collision between two billiard balls, in which all the momentum is transferred, and such a collision between nucleons could reproduce the main features of the reaction which we believe is due to charge exchange. However, such a picture requires the nuclear potential to be greater than the kinetic energy of the incident nucleon. There is in fact believed to be such a "hard core" potential, but it would have to extend to a radius larger than is usually assumed if it is to explain the relatively frequent occurrence of the reaction discussed here.

There are several possible reasons for the wider energy spectrum, which are connected mainly with the simplifications used in tackling the three body problem:-

- (i) G-B used the Born approximation, which is not very accurate in this intermediate energy range around 90 Mev.
- (ii) G-B say that their calculations are only rough, and they do not include any triplet state proton pairs in their analysis, simply

stating that any effect due to $\ell=1$ proton pairs will be small. If charge exchange were more likely without spin exchange than with it, then $\ell=1$ states would assume more importance, and would give a wider energy spectrum.

- (iii) It is possible that with three particles, the wave function for the final state cannot be separated with sufficient accuracy into a function of the fast nucleon multiplied by a function of the two slow nucleons. It is also interesting to see the difference in the calculated energy spectrum, assuming different wave functions for the slow protons. On the graph showing the neutron energy spectrum according to G-B there is also plotted a spectrum using a "plane wave approximation" for the final state of the slow nucleons. This spectrum is very broad indeed, suggesting that care must be used in choosing approximations for the final state wave function since the results are so sensitive to the choice.
- (iv) The coulomb force has been neglected in this work, by using G-B's analysis of the n-d problem for thep-d problem. However, the coulomb energy of two protons separated by the radius of the deuteron is only a few hundred kilowolts, which is too small to produce the necessary widening of the energy spectrum merely by adding it to the energy in the spectrum of G-B.

In the present work, the reaction has been investigated by analysing the slow protons produced instead of the fast neutrons; this method appears to work quite well and is perhaps more accurate and more informative about the details of the reaction.

The most striking result is the disagreement between the energy spectrum of neutrons predicted by G-B, and our experimental results. Their calculations are admittedly simplified, expecially

by assuming that the two protons move slowly relative to each other. Since this appears not always to be the case, more exact calculations are needed. In addition, more experimental results would be useful, especially to establish the angular distribution of the two slow protons in their centre of mass.

A magnet cloud chamber would be of great help in doing this, so as to reduce the error in measuring the energy of the protons, to prevent favouring of lower energy events and to eliminate the quadratic ambiguity present in some of our events in which only one proton is seen to stop.

REFERENCES

Chew, G.F. (1950), Phys. Rev. 80, 196.

Chew, G.F. (1951), Phys. Rev. 84, 710.

Cowan, E.W. (1950), Rev. Sci. Ins. 21, 991.

Fermi, E. (1950), "Muclear Physics", Chicago Press.

Fireman, E.L. (1954), Phys. Rev. 94, 385.

Firth, D.R. (1959), Can. J. Phys. 37, 1074.

Gluckstern, R.L. and Bethe, H.A. (1951), Phys. Rev. 81, 761.

Hofmann, J.A. and Strauch K. (1953), Phys. Rev. 90, 449.

Langsdorf, A. (1939), Rev. Sci. Inst. 10, 91.

Migdal, A.B. (1955), J. Exptl. Theoret. Phys. U.S.S.R. 28, 3.

Needels, T.S. and Neilsen, C.E. (1950) Rev. Sci. Inst. 21, 976.

Powell, W.M. (1957), Rev. Sci. Inst. 28, 472.

Shutt, R.P. (1951), Rev. Sci. Inst 22, 730.

Slatis, H. (1957), Nuc. Inst. 1, 213.

Watson, K.M. (1952), Phys. Rev. <u>88</u>, 1163.

APPENDIX A

The method used to calculate the co-ordinates in three-dimensions from the measurements (x_1y_1) , (x_2y_2) on the film is described here for the ideal case with symmetry between the two lenses. Several different attempts were made before a manageable approach was found, although the principle of the method is simple and obvious.

In Fig. 7 let L_1 and L_2 be the lenses, O_1 and O_2 the feet of the perpendiculars from L_1 and L_2 onto the film planes which are inclined to the L_1L_2 or X-direction at an angle ϵ . Then the origin for (x_1y_1) is O_1 and for (x_2y_2) is O_2 , and the intersection of the light rays O_1L_1 and O_2L_2 is O_1 , the origin for (X Y Z). Let the focal distances O_1L_1 and O_2L_2 be f, L_1 $C = L_2C = A$ and OC = H. The glass has thickness t, refractive index n and is parallel to the X-Y plane.

P₁ and P₂ are the images of some point P which is not necessarily in the Y = O plane. Point L_1 has X = A, Y = O, Z = H, otherwise written (A, O, H).

If the direction cosines of P₁L₁ are $(\lambda_1 \ \mu_1 \ \nu_1)$, the line P₁L₁ is:-

$$\frac{X - A}{\lambda_1} = \frac{Y}{\mu_1} = \frac{Z - H}{\nu_1}$$

This ray strikes the top surface at (X¹, Y¹, D) given by:-

$$\frac{\underline{X}^{\dagger} - \underline{A}}{\lambda_{1}} = \frac{\underline{Y}^{\dagger}}{\mu_{1}} = \frac{\underline{D} - \underline{H}}{\nu_{1}}$$

and the equation of the ray in the glass is:-

$$\frac{X - X^{t}}{\lambda_{1}^{t}} = \frac{Y - Y^{t}}{\mu_{1}^{t}} = \frac{Z - D}{\nu_{1}^{t}}$$

where $(\lambda_1^i, \mu_1^i \nu_1^i)$ are the direction cosines given by the lens of refraction as

$$\lambda^{t} = \frac{\lambda}{n} \qquad \mu^{t} = \frac{\mu}{n} \qquad 1 - \nu^{t^{2}} = \frac{1 - \nu^{2}}{n^{2}}$$

The ray in the glass leaves the bottom surface at $(X^{"}, Y^{"}, D-t)$ given by:-

$$\frac{\underline{x}^{n} - \underline{x}^{t}}{\lambda_{1}^{t}} = \frac{\underline{y}^{n} - \underline{y}^{t}}{\mu_{1}^{t}} = \frac{(\underline{D} - \underline{t}) - \underline{D}}{\nu_{1}^{t}}$$

and the equation of the ray in the cloud chamber is therefore:-

$$\frac{\mathbf{X} - \mathbf{X}''}{\lambda_{1}} = \frac{\mathbf{Y} - \mathbf{Y}''}{\mu_{1}} = \frac{\mathbf{Z} - (\mathbf{D} - \mathbf{t})}{\nu_{1}}$$

After eliminating X^{\dagger} , Y^{\dagger} , Z^{\dagger} , $X^{"}$, $Y^{"}$, $Z^{"}$, and D (which drops out, as expected, since only the thickness of the glass should matter, not its height) one finds the equations

$$\frac{X-A}{\lambda_1} + \frac{t}{\nu_1}, \frac{\lambda_1}{\lambda_1} = \frac{Y}{\mu_1} + \frac{t}{\nu_1}, \frac{\mu_1}{\mu_1} = \frac{Z-H}{\nu_1} + \frac{t}{\nu_1}$$

If t = 0, or n = 1, the equations for the ray above the glass are reproduced as they must.

The ray from P_2 is given by writing -A for A and changing subscripts from 1 to 2.

We therefore have four equations to find X Y Z; the determinant of the 4 x 4 matrix gives the Δ -condition.

There is more than one way of solving such a set of equations, and one chooses not necessarily the algebraically simplest but the one which will be the most accurate bearing in mind that the $\lambda^{\dagger}s$ have to be found from measurements.

The solutions finally used were:-

$$2A = (Z-H)(\frac{\lambda_{2}}{\nu_{2}} - \frac{\lambda_{1}}{\nu_{1}}) + t\left[(\frac{\lambda_{2}}{\nu_{2}} - \frac{\lambda_{1}}{\nu_{1}}) - (\frac{\lambda_{2}}{\nu_{2}^{2} + n^{2} - 1} - \frac{\lambda_{1}}{\sqrt{\nu_{1}^{2} + n^{2} - 1}})\right]$$

$$2Y = (Z-H)(\frac{\mu_{2}}{\nu_{2}} + \frac{\mu_{1}}{\nu_{1}}) + t\left[(\frac{\mu_{2}}{\nu_{2}} + \frac{\mu_{1}}{\nu_{1}}) - (\frac{\mu_{2}}{\sqrt{(2)}} + \frac{\mu_{1}}{\sqrt{(1)}})\right]$$

$$2X = (Z-H)(\frac{\lambda_{2}}{\nu_{2}} + \frac{\lambda_{1}}{\nu_{1}}) + t\left[(\frac{\lambda_{2}}{\nu_{2}} + \frac{\lambda_{1}}{\nu_{1}}) - (\frac{\lambda_{2}}{\sqrt{(2)}} + \frac{\lambda_{1}}{\sqrt{(1)}})\right]$$

The determinant gives:

$$2A \left(\frac{\nu_2}{\mu_2} - \frac{\nu_1}{\mu_1}\right) = t \left(\frac{\lambda_2}{\mu_2} - \frac{\lambda_1}{\mu_1}\right) \left(\frac{\nu_1}{\sqrt{(1)}} - \frac{\nu_2}{\sqrt{(2)}}\right).$$

The equations yield simple forms if t = 0 or n = 1. In particular the determinant equation gives $\frac{\nu_2}{\mu_2} = \frac{\nu_1}{\mu_1}$, which is just the condition that the rays projected onto the Y-Z plane should be the hypoteneuse of the same triangle.

That the determinant is related to the least distance between the lines may be seen most easily by use of the equation in vector form.

Let the equations of the two rays be
$$\underline{r} = \underline{r}_1 + s \underline{n}_1$$

 $\underline{r} = \underline{r}_2 + t \underline{n}_2$

where for example \underline{r}_1 is any point on line one and \underline{n}_1 is the unit vector in the direction of line one. s and t are distances along the lines.

If these meet in space, there is a pair of (s, t) say (s_o, t_o) satisfying $\underline{r}_1 + s_o \underline{n}_1 = \underline{r}_2 + t_o \underline{n}_2$. Thus we have three equations (for the three components) and only two unknowns s_o and t_o, so that a restriction appears on the \underline{r}_1 , \underline{r}_2 , \underline{n}_1 , \underline{n}_2 . This restriction is $\Delta = 0$, provided the lines actually do meet. If they do not meet, the same function of $(\underline{r}_1, \underline{r}_2, \underline{n}_1, \underline{n}_2)$ is no longer zero, but is related to the minimum distance between the lines:-

 Δ is got by eliminating s and t from

 $0 = (\underline{r}_1 - \underline{r}_2) + s \underline{n}_1 - t \underline{n}_2; \text{ by using components or multi-}$ plying by \underline{n}_1 , \underline{n}_2 , or $\underline{n}_1 \times \underline{n}_2$ one easily sees that,

$$\Delta = (\underline{\mathbf{r}}_1 - \underline{\mathbf{r}}_2) \cdot (\underline{\mathbf{n}}_1 \times \underline{\mathbf{n}}_2).$$

Now consider $\underline{\omega} = (\underline{r}_1 - \underline{r}_2) + s \underline{n}_1 - t \underline{n}_2$, where $\underline{\omega}$ is the distance between two points s and t, one on each line.

Form the unit vector $\underline{\mathbf{m}} = \frac{\underline{\mathbf{n}_1} \times \underline{\mathbf{n}_2}}{\underline{\mathbf{n}_1} \times \underline{\mathbf{n}_2}}$ perpendicular to $\underline{\mathbf{n}}$ and $\underline{\mathbf{n}_2}$.

Now the minimum vector $\underline{\omega}_{\underline{\mathbf{m}}}$ has the direction of $\underline{\mathbf{m}}$ therefore $\underline{\omega}_{\underline{\mathbf{m}}} = \underline{\mathbf{m}} \cdot (\underline{\mathbf{r}_1} - \underline{\mathbf{r}_2})$, from multiplying the equation for $\underline{\omega}$ by $\underline{\mathbf{m}}$. Hence,

$$\Delta = \omega_{m} / \underline{n}_{1} \times \underline{n}_{2} /$$
or
$$\Delta^{2} = \omega_{m}^{2} (1 - (\underline{n}_{1} \cdot \underline{n}_{2})^{2}) = \omega_{m}^{2} \sin^{2} \alpha,$$

where a is the angle between the rays.

With three cameras, there would be three Δ^{ϵ} s and one could arrange to minimise a suitable combination of these Δ^{ϵ} s.

We still have to find the direction cosines in terms of the (x_1y_1) and (x_2y_2) and the camera constants. They are:-

$$(\lambda_{1}, \mu_{1}, \nu_{1}) = \frac{1}{\sqrt{1 + (\frac{x}{f_{1}})^{2} + (\frac{y}{f_{1}})^{2}}} (\sin \epsilon - \frac{x_{1}}{f_{1}} \cos \epsilon, \frac{-y_{1}}{f_{1}}, \cos \epsilon + \frac{x_{1}}{f_{1}} \sin \epsilon)$$

For the $(\lambda_2, \mu_2, \nu_2)$ one changes subscripts and writes $-\epsilon$ for ϵ . In actual fact the problem is not as symmetrical as this. The origin actually used is not at the intersection of the rays 0_1 L₁ and 0_2 L₂. Taking into account this and other differences the direction cosines become:

$$(\lambda, \mu, \nu) = \frac{1}{\sqrt{1 + (\frac{x}{f} + \beta)^2 + (\frac{y}{f})^2}} \quad (\pm \sin \epsilon - (\frac{x}{f} + \beta)\cos \epsilon, \frac{y}{f}, \cos \epsilon \pm (\frac{x}{f} + \beta) \sin \epsilon)$$

Take + sign with subscript 1

- sign with subscript 2.

The β 's are camera constants representing the angle between the ray through L from the ideal origin and the ray from the actual fiducial mark used as origin. Tilting of the glass with respect to the X-Y plane was ignored; the correction introduced by the glass is surprisingly small anyway.

The equations giving X Y Z are also altered by the fact that L_1 C does not equal L_2 C. Calling L_1 C = A_1 L_1 C = A_2 and with a rearrangement to help computation:-

$$\begin{aligned} (\mathbb{A}_{1} + \mathbb{A}_{2}) \ \mathcal{V}_{1} \ \mathcal{V}_{2} &= \ (\mathbb{Z} - \mathbb{H}) \left(\lambda_{2} \mathcal{V}_{1} - \lambda_{1} \mathcal{V}_{2} \right) \ + \ \mathbf{t} \left[\left(\lambda_{2} \mathcal{V}_{1} - \lambda_{1} \mathcal{V}_{2} \right) \ - \ \mathcal{V}_{1} \ \mathcal{V}_{2} \ \left(\frac{\lambda_{2}}{\sqrt{(2)}} - \frac{\lambda_{1}}{\sqrt{(1)}} \right) \ \right] \\ & 2 \mathbb{Y} \ \mathcal{V}_{1} \ \mathcal{V}_{2} &= \ (\mathbb{Z} - \mathbb{H}) \left(\mu_{2} \mathcal{V}_{1} - \mu_{1} \mathcal{V}_{2} \right) \ + \ \mathbf{t} \left[\left(\mu_{2} \mathcal{V}_{1} + \mu_{1} \mathcal{V}_{2} \right) \ - \ \mathcal{V}_{1} \ \mathcal{V}_{2} \ \left(\frac{\mu_{2}}{\sqrt{(2)}} - \frac{\mu_{1}}{\sqrt{(1)}} \right) \right] \\ & 2 \mathbb{X} \ + \left(\mathbb{A}_{2} - \mathbb{A}_{1} \right) \ = \ (\mathbb{Z} - \mathbb{H}) \left(\lambda_{2} \mathcal{V}_{1} + \lambda_{1} \mathcal{V}_{2} \right) \ + \ \mathbf{t} \left[\left(\lambda_{2} \mathcal{V}_{1} + \lambda_{1} \mathcal{V}_{2} \right) \ - \ \mathcal{V}_{1} \ \mathcal{V}_{2} \ \left(\frac{\lambda_{2}}{\sqrt{(2)}} - \frac{\lambda_{1}}{\sqrt{(1)}} \right) \right] \\ & \Delta \ = \ \left(\mu_{2} \mathcal{V}_{1} - \mu_{1} \mathcal{V}_{2} \right) \ + \ \frac{\mathbf{t}}{\left(\mathbb{A}_{1} + \mathbb{A}_{2} \right)} \ \left(\mu_{1} \lambda_{2} - \mu_{2} \lambda_{1} \right) \left(\frac{\mathcal{V}_{1}}{\sqrt{(1)}} - \frac{\mathcal{V}_{2}}{\sqrt{(2)}} \right) \end{aligned}$$

The equations in this form restrict the size of every term involving direction cosines to less than two, and so are ideal for fixed point programming.

The value of H is determined in terms of the other camera constants by putting $x_1 = y_1 = x_2 = y_2 = 0$.

Rotation into beam co-ordinate system

If the direction cosines of a line relative to the camera axes are (α, β, γ) , and the incident beam relative to these axes has direction cosines (a, b, c) then we rotate into a system such that the incident direction is the new X-axis, and the new Y-axis is in the plane of the old Y-axis and the incident proton direction.

The transformation equations are

$$(\lambda, \mu, \nu) = (a\alpha + b\beta + c\gamma, -\frac{b\alpha + a\beta}{\sqrt{a^2 + b^2}}, -\frac{c(a\alpha + b\beta)}{\sqrt{a^2 + b^2}} + \gamma \sqrt{a^2 + b^2}),$$

where (λ, μ, ν) are the direction cosines of a track in the new system of axes.

Criteria for optimising camera constants

To ensure that the six fiducial marks lie in a plane it is not enough to minimise $\sum_{i=1}^{3} (\underline{r}_{i} + \underline{r}_{i+3})^{2}$, as this allows buckling perpendicular to the plane of the hexagon.

However, if three vectors $\underline{\mathbf{r}}_1$, $\underline{\mathbf{r}}_2$ and $\underline{\mathbf{r}}_3$ are coplanar then $(\underline{\mathbf{r}}_1 \wedge \underline{\mathbf{r}}_3) \cdot \underline{\mathbf{r}}_2 = 0$ and a sum of squares of this quantity could be minimised.

Similarly $(\underline{r}_1 \times \underline{r}_2) \cdot (\underline{r}_2 \times \underline{r}_3) - \frac{3}{4} R^4 = 0$ if all lie in a plane and this expression reduces to

$$(\underline{\mathbf{r}}_1 \cdot \underline{\mathbf{r}}_3) \ \mathbf{r}_2^2 - (\underline{\mathbf{r}}_1 \cdot \underline{\mathbf{r}}_2) (\underline{\mathbf{r}}_2 \cdot \underline{\mathbf{r}}_3) - \frac{3}{4} \ \mathbf{R}^4 = 0$$

which contains simple terms easily evaluated.

In a similar way other arrays of fiducial marks can be used, preferably extending in three dimensions.

APPENDIX B

Kinematics of the event

Momentum of non-stopping proton

In calculating the kinematics, it was found best to use direction cosines and relative momenta in most cases, and to use vectors for the remainder. By relative momentum \underline{x} we mean $\underline{x} = p/p_0$.

Let \underline{p} be the incident proton momentum

p be the neutron momentum

 $\underline{\mathbf{p}}_1$ and $\underline{\mathbf{p}}_2$ be the slow proton momenta.

So $\underline{p}_0 = \underline{p} + \underline{p}_1 + \underline{p}_2$ by conservation of momentum, and $\underline{p}_0^2 = \underline{p}^2 + \underline{p}_1^2 + \underline{p}_2^2 + \underline{q}^2$ by energy conservation.

Naturally q^2 represents the binding energy of the deuteron, and we also define $k^2 = \frac{1}{2} \; q^2/p_o^2$.

Using $\underline{p} = \underline{p}_0 - (\underline{p}_1 + \underline{p}_2)$ in the energy equation to eliminate \underline{p}^2 , we get

$$p_1^2 + p_2^2 = p_0 \cdot (p_1 + p_2) - p_1 \cdot p_2 - \frac{1}{2} q^2$$

Translating this into relative momenta gives

$$x_1^2 + x_2^2 = \lambda_1 x_1 + \lambda_2 x_2 - x_1 x_2 \cos \alpha - k^2$$

 λ_1 and λ_2 are the direction cosines of \underline{p}_1 and \underline{p}_2 relative to \underline{p}_0 and $\cos \alpha$ is the angle between \underline{p}_1 and \underline{p}_2 .

This is the equation used to find the unknown x_1 if x_2 and all direction cosines of the protons are known. A rather unexpected feature was the importance of the binding energy term k^2 , which is comparable with the x_1^2 and x_2^2 in many cases.

It had seemed intuitively reasonable that the binding energy of 2.2 Mev could be neglected in comparison with the incident proton

energy of 90 Mev, and therefore that it might be neglected entirely.

On rewriting as

$$x_1^2 - (\lambda_1 - x_2 \cos \alpha) x_1 + x_2^2 + k^2 - \lambda_2 x_2 = 0$$

the two solutions are obviously

$$2x_1 = (\lambda_1 - x_2 \cos \alpha) \pm \sqrt{(\lambda_1 - x_2 \cos \alpha)^2 + 4(\lambda_2 x_2 - x_2^2 - k^2)}$$

and the conditions under which both roots (if real) are positive is

$$\lambda_1 - x_2 \cos \alpha > 0$$

$$x_2^2 + k^2 - \lambda_2 x_2 > 0$$

Energy and angle of neutron

The energy of the neutron is $p_0^2 \left[1 - (x_1^2 + x_2^2 + 2k^2)\right]$ but it is of more interest to use $p_0^2(x_1^2 + x_2^2)$, the energy of the two protons.

The angle \emptyset which the neutron makes with the incident direction is found as follows:

$$\cos \emptyset = \frac{\underline{p}_0 \cdot \underline{p}}{\underline{p}_0 \underline{p}}$$

Multiply the momentum equation by \underline{p}_{o} giving,

$$p_0^2 = p_0 \cdot p + p_0 \cdot (p_1 + p_2)$$
 or $p_0 \cdot p = p_0^2 - p_0 \cdot (p_1 + p_2)$

The energy equation gives $p^2 = p_0^2 - p_1^2 + p_2^2 + q^2$

$$\cos \emptyset = \frac{p_0^2 - p_0 \cdot (p_1 + p_2)}{p_0 \left[p_0^2 - (p_1^2 + p_2^2 + q^2)\right]} \frac{1}{2}$$

In terms of relative momenta and direction cosines,

$$\cos \emptyset = \frac{1 - (\lambda_1 x_1 + \lambda_2 x_2)}{\left[1 - (x_1^2 + x_2^2 + 2k^2)\right]^{1/2}}$$

There is an alternate form which involves only invariant quantities x_1x_2 and $\cos \alpha$, (if we know them independently), which is obtained by using $\lambda_1x_1 + \lambda_2x_2$ from the quadratic form for x_1 and x_2 :

$$\cos \emptyset = \frac{1 - (x_1^2 + x_2^2 + k^2 + x_1 x_2 \cos \alpha)}{\left[1 - (x_1^2 + x_2^2 + 2k^2)\right]^{1/2}}$$

Centre of mass transformation

The momentum of a proton in the centre of mass of the two protons is $\pm \underline{p}^{t}$ where $\underline{p}^{t} = \frac{1}{2}(\underline{p}_{1} - \underline{p}_{2})$ or relatively

$$\underline{x}^{1} = \frac{1}{2} (\underline{x}_{1} - \underline{x}_{2}).$$

The direction cosines of \underline{p}^{t} measured relative to the laboratory system are obviously

$$(\lambda^{i}, \mu^{i}, \nu^{i}) = \frac{1}{\left[x_{1}^{2} + x_{2}^{2} - 2x_{1}x_{2} \cos \alpha\right]^{1/2}} (\lambda_{1}x_{1}^{-\lambda_{2}}x_{2}^{2}, \mu_{1}\lambda_{1}^{-\mu_{2}}x_{2}^{2}, \mu_{1}\lambda_{1}^{-\mu_{2}}x_{2}^{2})$$
and $x^{i^{2}} = \frac{1}{4} (x_{1}^{2} + x_{2}^{2} - 2x_{1}x_{2}^{2} \cos \alpha).$

As described in the kinematic chapter, one must now find the direction of \underline{x}^1 in a frame of reference with unit vectors $(\underline{y},\underline{y},\underline{y})$ in directions $(\underline{P} \times (\underline{P} \times \underline{p}_0), \underline{P}, \underline{P} \times \underline{p}_0)$ respectively, where $\underline{P} = \underline{p}_1 + \underline{p}_2$. This calculation was done by finding the nine direction cosines of \underline{y} , \underline{y} , and \underline{y} in the laboratory frame. One starts by finding direction cosines of \underline{P} which are

(A, B, C) =
$$\frac{1}{\left[x_1^2 + x_2^2 + 2x_1 x_2 \cos \alpha\right]} \frac{1}{2} (\lambda_1 x_1^2 + \lambda_2 x_2, \mu_1 x_1^2 + \mu_2 x_2, \mu_1 x_1^2 + \mu_2 x_2)$$

The direction cosines of \sum and \sum are simple functions of (A, B, C) because in the laboratory frame p_0 has directions (1, 0, 0).

Finally the formulae for directions in the scattering frame are:-

$$(\ell, m, n) = \frac{-\lambda'(B^2 + C^2) + \mu'AB + \nu'AC}{\left[B^2 + C^2\right]^{1/2}}, \frac{\mu'C - \nu'B}{\left[B^2 + C^2\right]^{1/2}}, \lambda'A + \mu'B + \nu'C).$$

APPENDIX C

Energy Spectrum in Centre of Mass

With the assumptions made in the discussion about the neutron energy spectrum one can write the probability of a neutron in $d\lambda$ at λ and dx^2 at x^2 as

$$f(\lambda) g (x_m^2 - x^2) d\lambda dx^2$$
,

where x_m^2 is the maximum neutron energy kinematically possible at an angle λ .

For a given x^2 , λ we now find the energy in the C.M. of the two protons:-

$$2\underline{\mathbf{x}}^{\mathbf{i}} = \underline{\mathbf{x}}_{1} - \underline{\mathbf{x}}_{2}$$

$$4\mathbf{x}^{\mathbf{i}^{2}} = \mathbf{x}_{1}^{2} + \mathbf{x}_{2}^{2} - 2\underline{\mathbf{x}}_{1} \cdot \underline{\mathbf{x}}_{2}$$

therefore

The conservation of momentum gives $\underline{i}_0 = \underline{x}_1 + \underline{x}_2 + \underline{x}$ where \underline{i}_0 is the unit vector in the direction \underline{p}_0 so that

$$(\underline{i}_0 - \underline{x})^2 = (x_1 + \underline{x}_2)^2$$

$$1 - 2\lambda x + x^2 = x_1^2 + x_2^2 + 2\underline{x}_1 \cdot \underline{x}_2$$

or

Using this to eliminate $2\underline{x}_1 \cdot \underline{x}_2$ from the last equation for $4x^{1/2}$ gives

$$(1 - 2\lambda x + x^2) + 4x^{2} = 2(x_1^2 + x_2^2).$$

Energy conservation, $1 = x_1^2 + x_2^2 + x^2 + 2k^2$ allows elimination of $x_1^2 + x_2^2$ giving $4(x_1^2 + k^2) = 1 + 2\lambda x - 3x^2$.

This equation shows that the maximum x (for a given λ) occurs when $x^2 = 0$, or $\underline{p}_1 = \underline{p}_2$ as stated in the discussion.

Thus $4k^2 = 1 + 2\lambda x_m - 3x_m^2$ and by subtracting this from the equation with x^2 not equal to zero,

$$4x^{2^{2}} = 2\lambda (x - x_{m}) - 3(x^{2} - x_{m}^{2})$$
$$= (3 - \frac{2\lambda}{x + x_{m}})(x_{m}^{2} - x^{2}).$$

Now for a neutron spectrum 5 MeV wide at 100 MeV, $\frac{x_m}{x}$ 1.03, and also $\frac{x_m}{x}$ only goes from 1 to 1.03 as the neutron angle changes from 0° to 30°. Thus with an error of 5% at the most we can write:-

$$4x^{1/2} \approx 2(x_{\rm m}^2 - x^2),$$

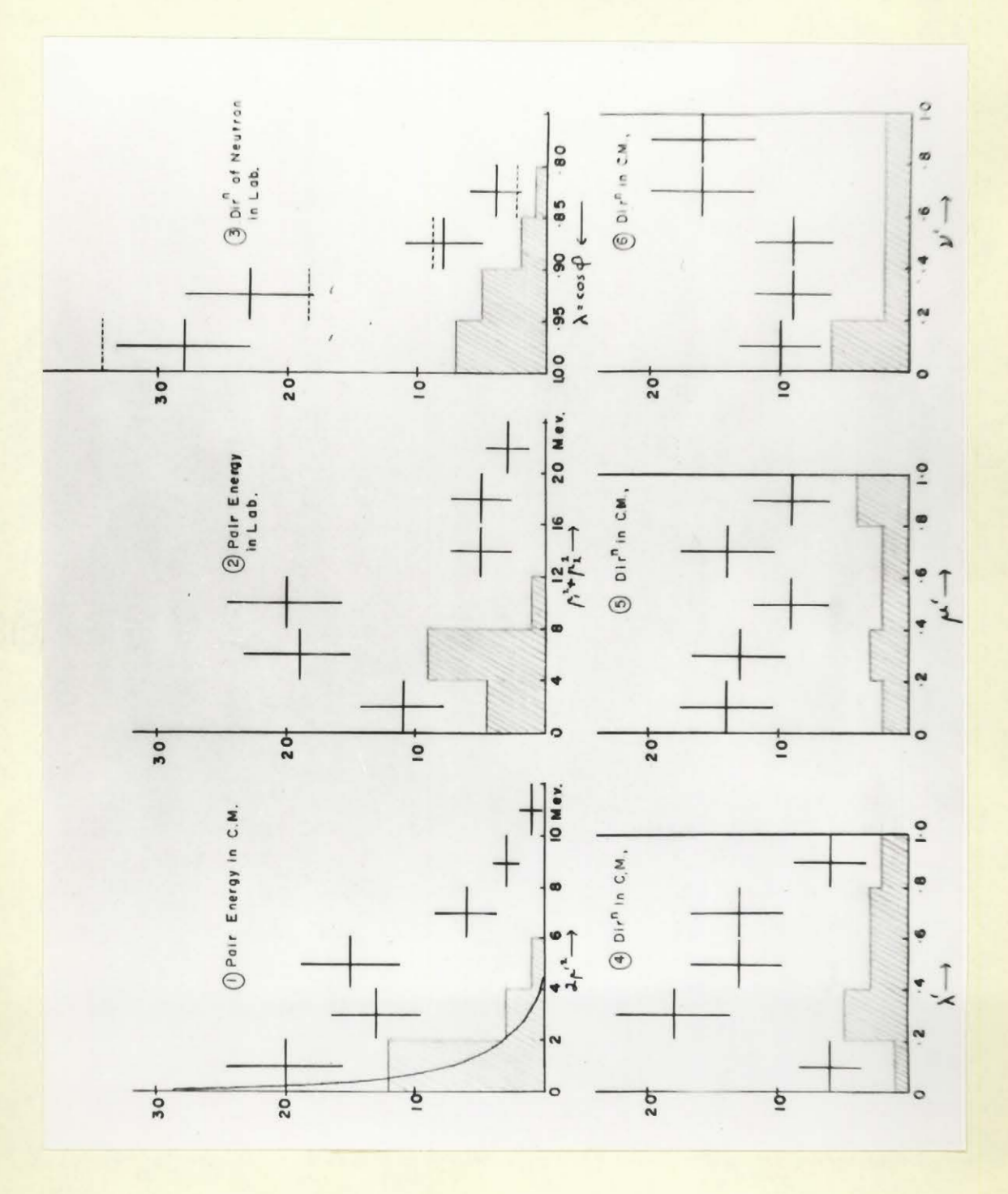
or calling the C.M. energy $2x^{2} = 5^2$

$$\xi^2 \simeq (x_m^2 - x^2)$$

where ξ^2 is independent of λ . Hence $d\xi^2 = -dx^2$ and the distribution of C.M. energies is

$$f(\lambda) g(\xi^2) d\lambda d\xi^2$$
.

We can now integrate over λ , and writing $\int f(\lambda) d\lambda = F$, the probability of ξ^2 in $d\xi^2$ is $F g(\xi^2) d\xi^2$, which is the same form as the neutron energy spectrum at a single angle only.



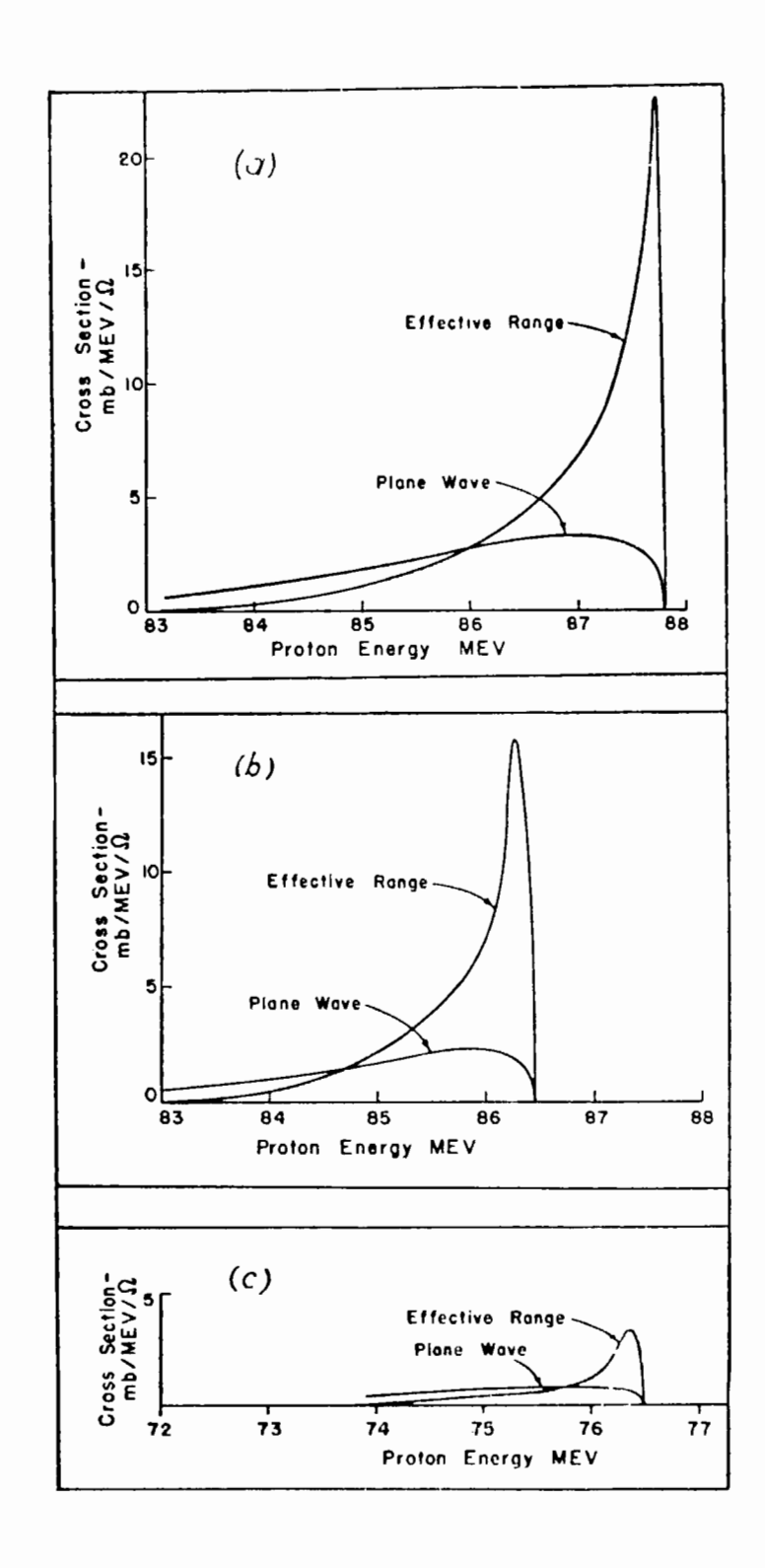


Fig.1 - Fast nucleon energy spectrum according to G - B.

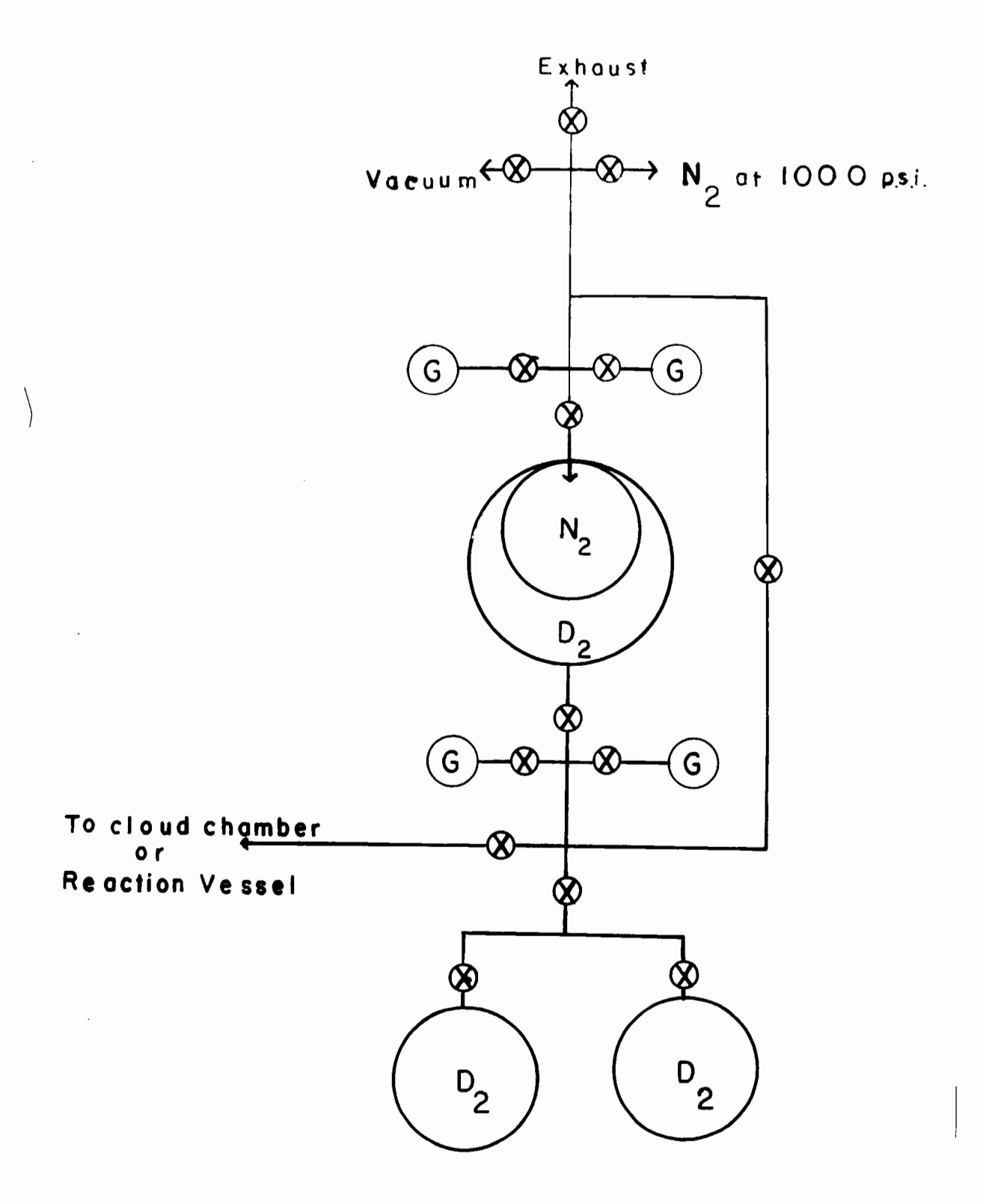


FIG. 2

Fig.2 - Deuterium pumping system

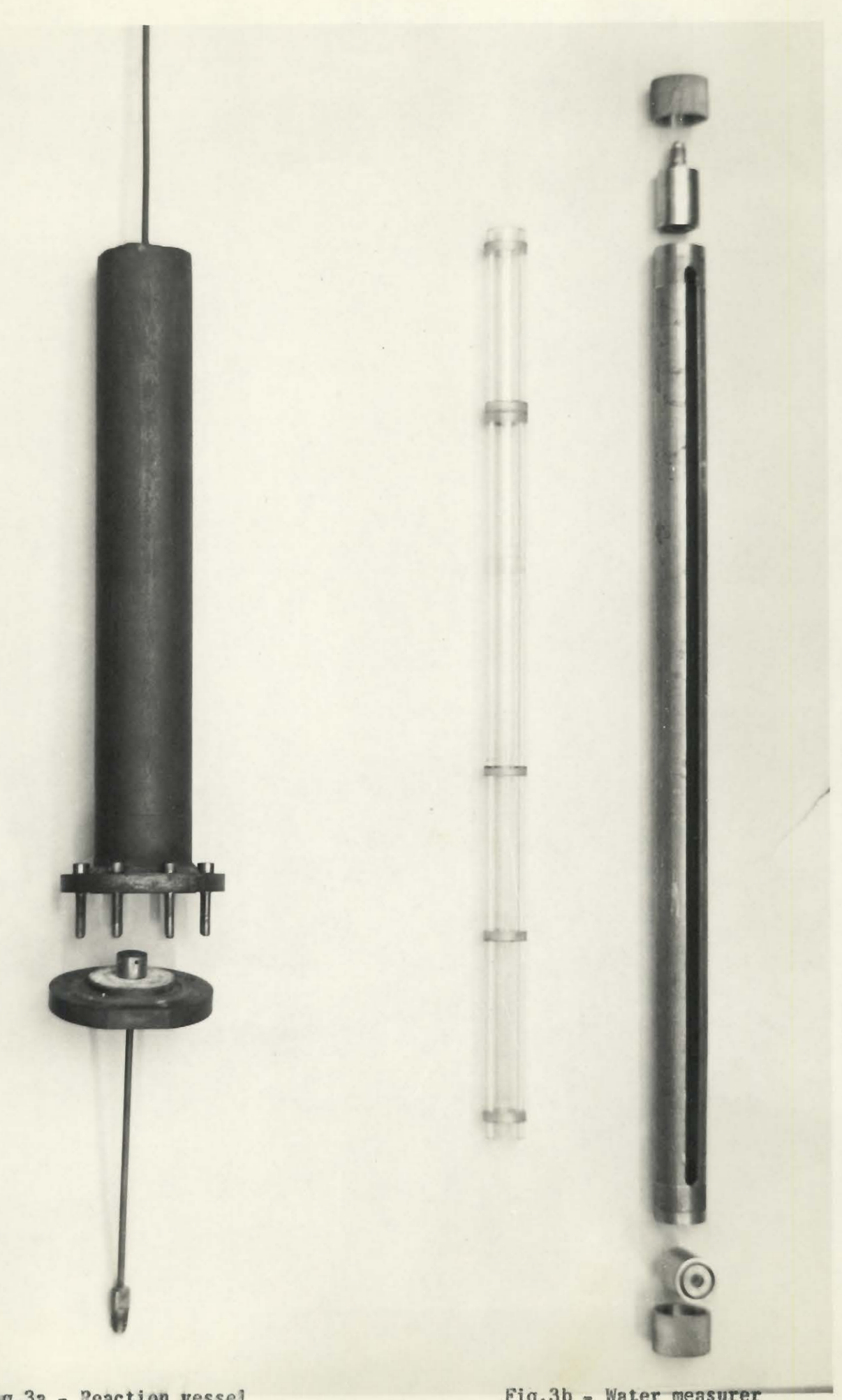


Fig.3a - Reaction vessel

Fig.3b - Water measurer

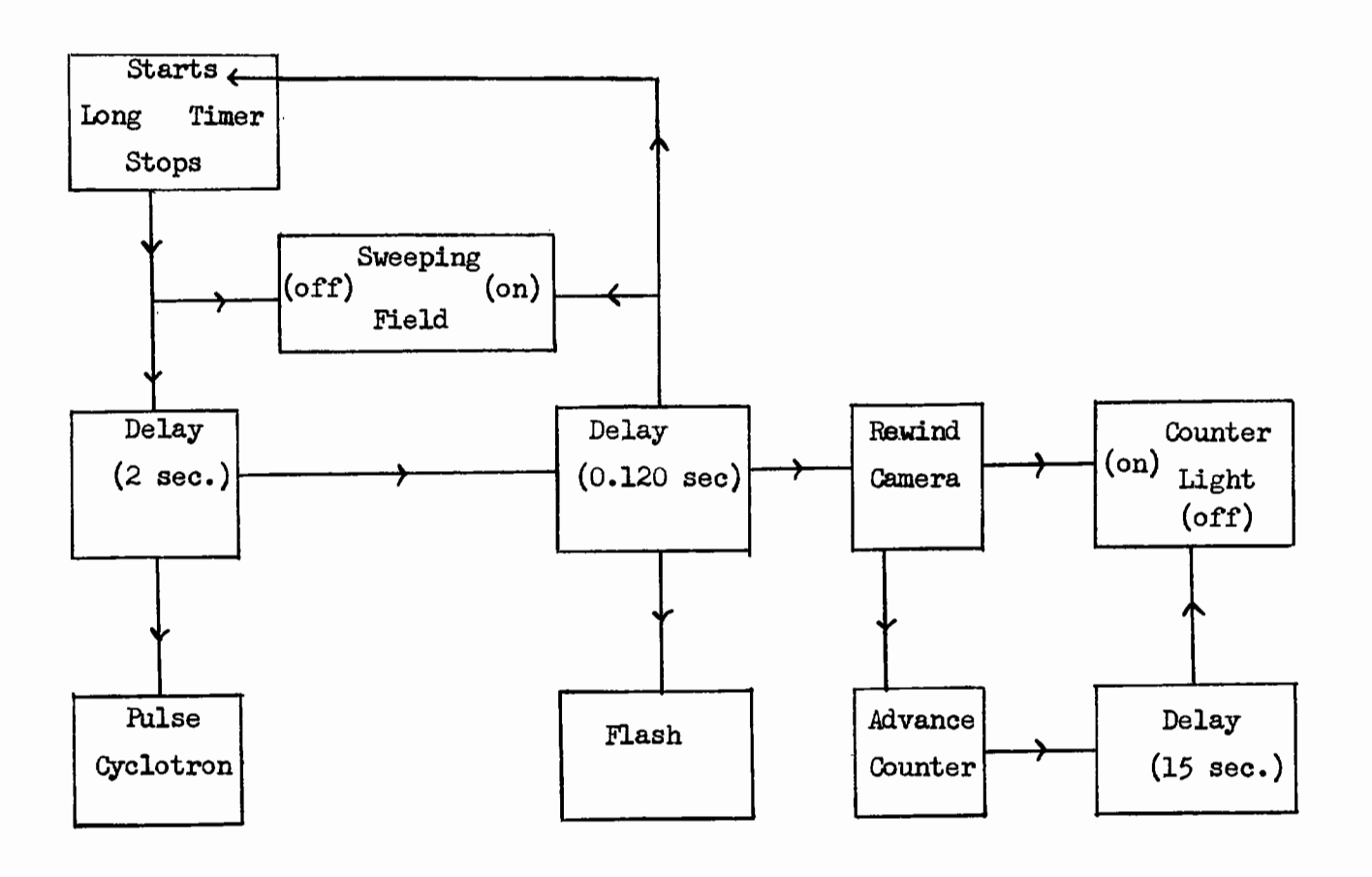


Fig. 4 CONTROL FUNCTIONS

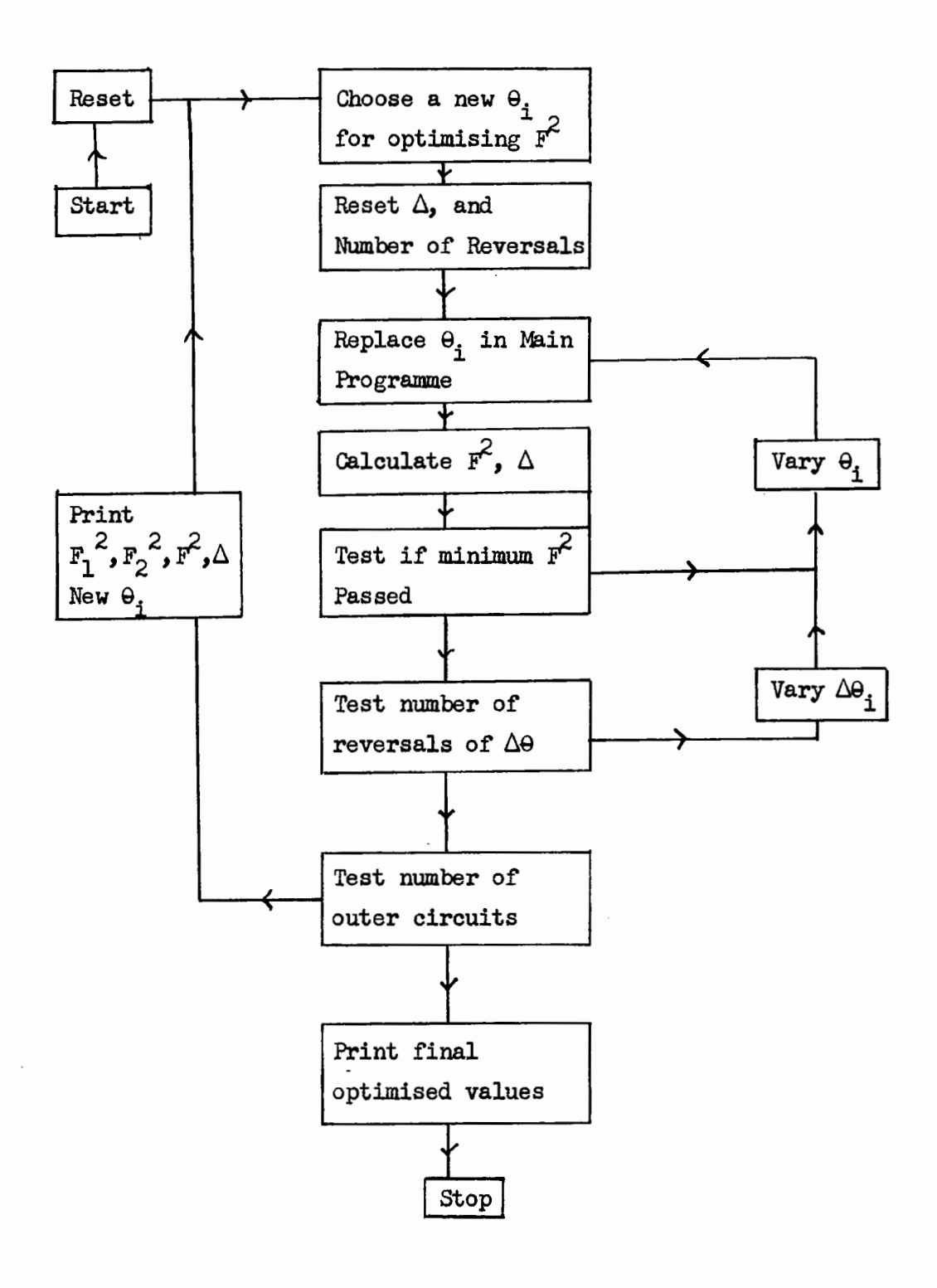


Fig. 5 OPTIMISING PROGRAMME

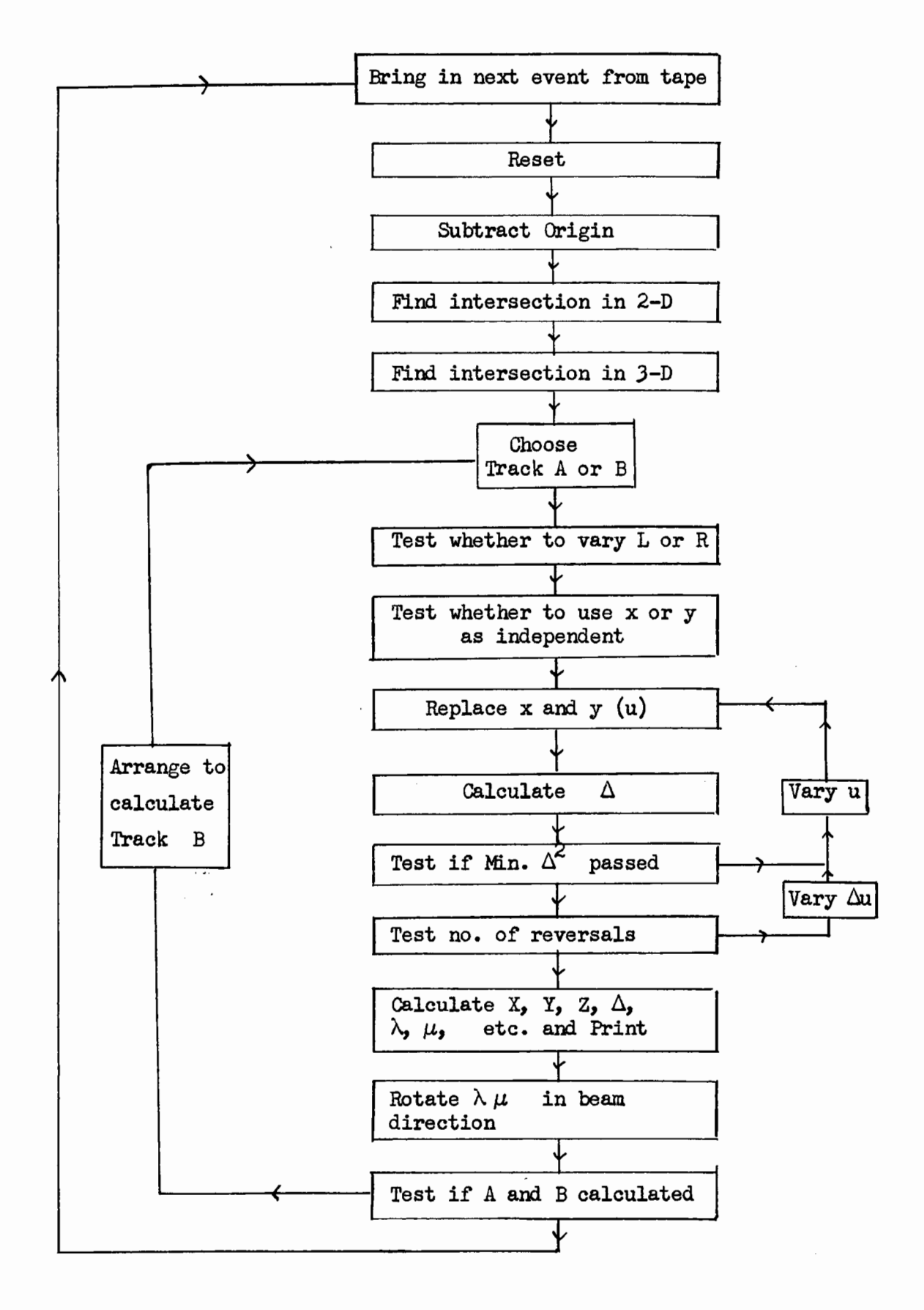
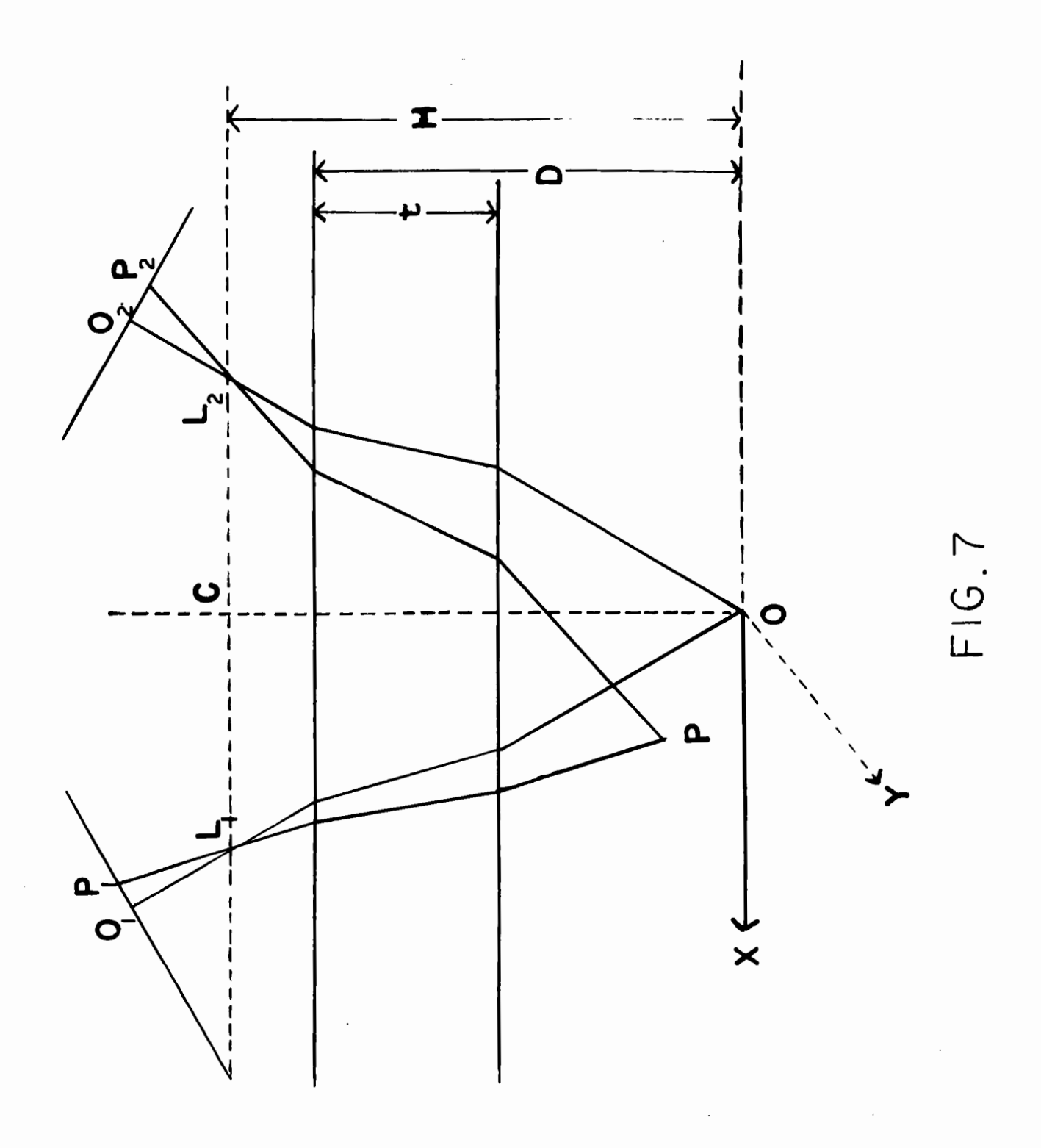


Fig. 6 EVENT PROGRAMME



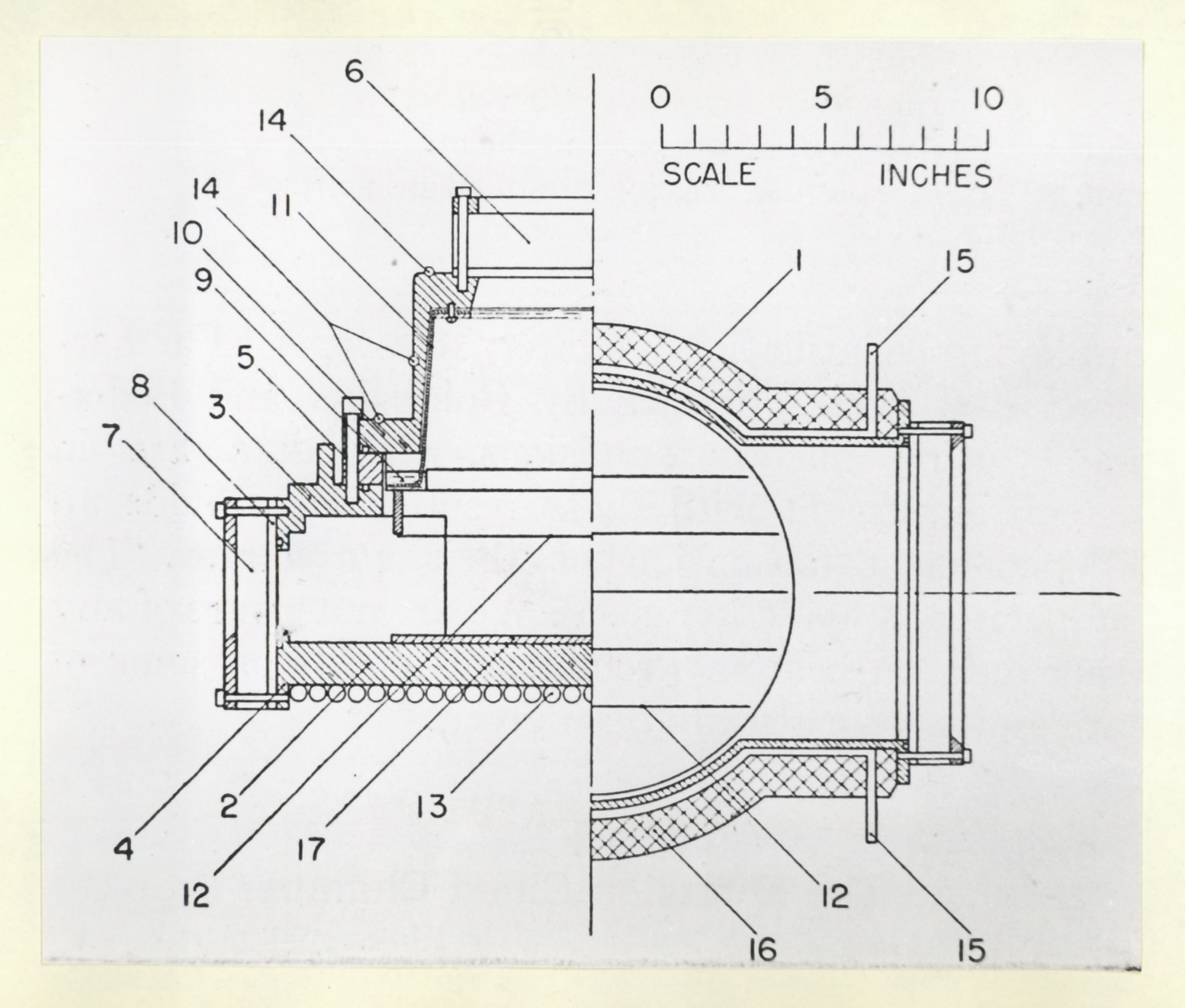


Fig.8 - Chamber section

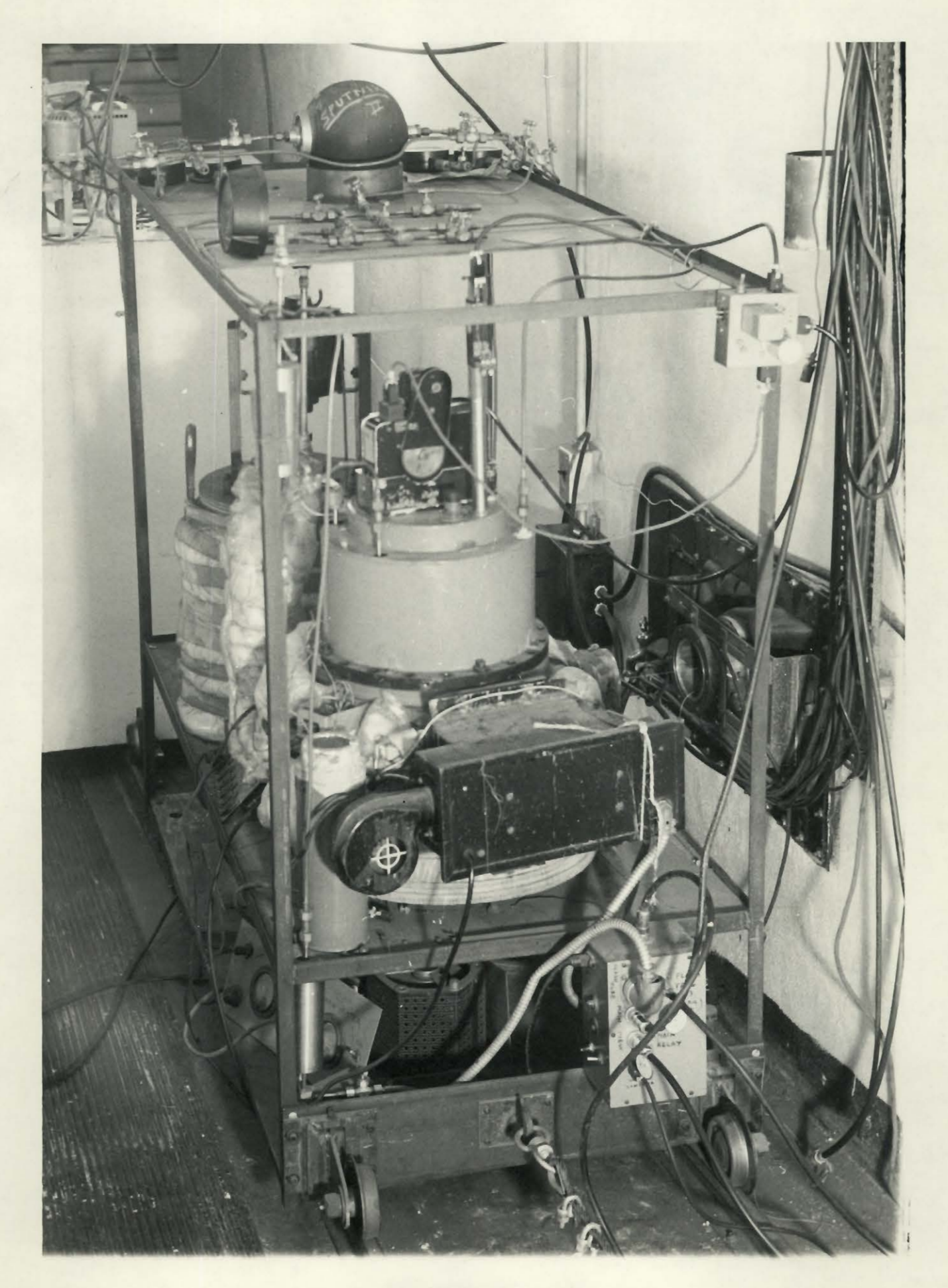


Fig.9 - General view of apparatus

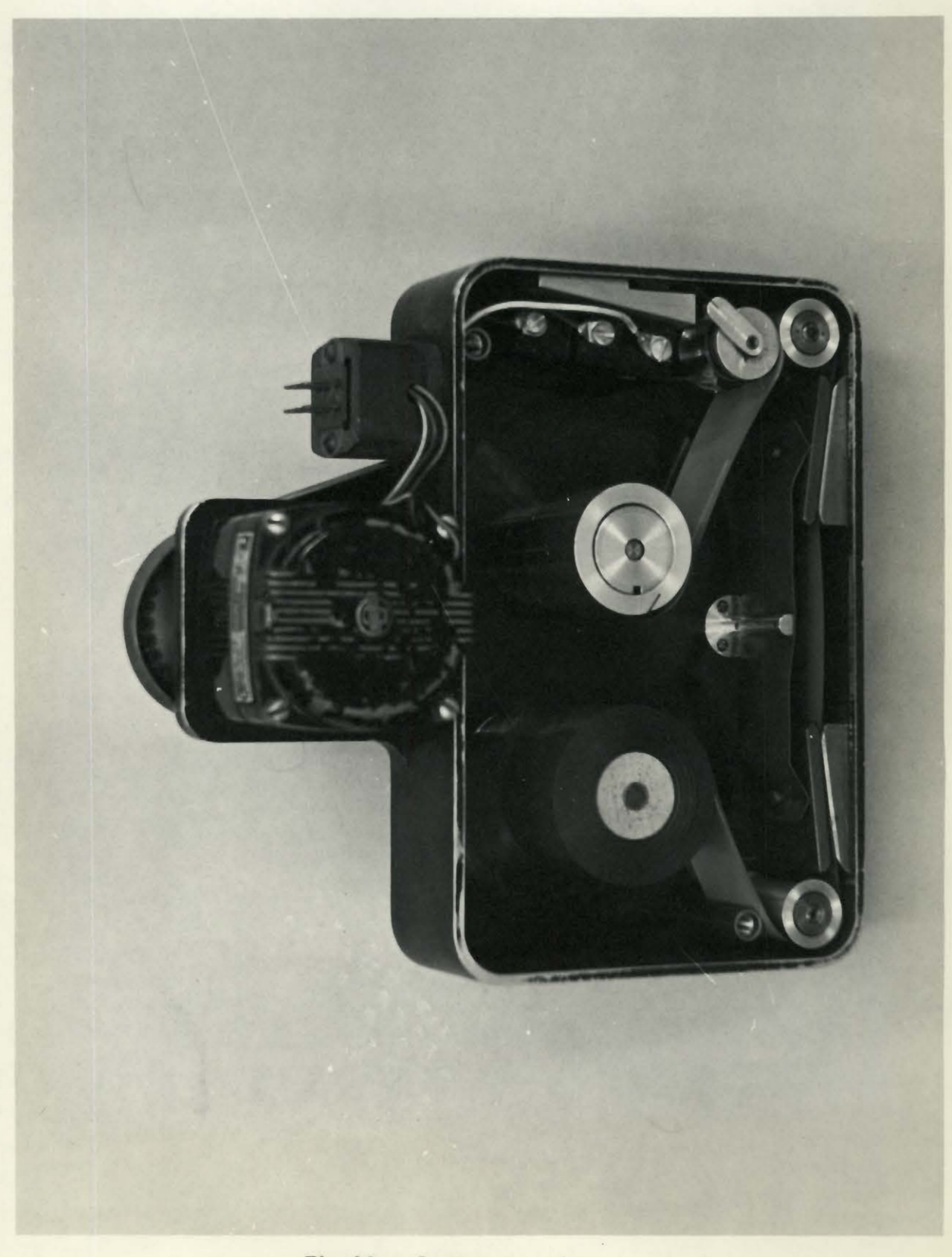
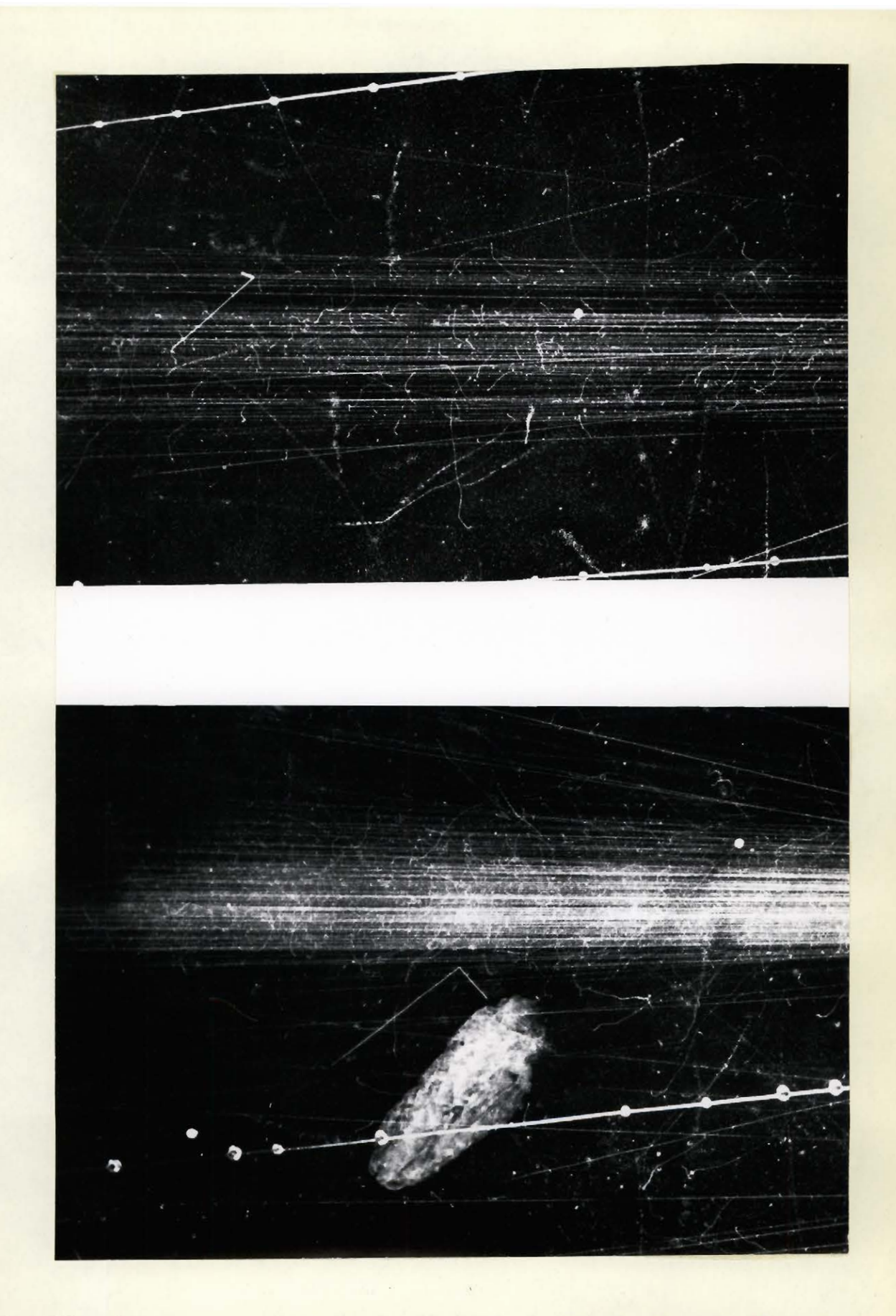


Fig. 10 - Camera magazine



Figs.11 and 12 - Examples of slow proton pairs. (In fig.12, note formation of cloud in sensitive region caused by drop falling to bottom of chamber.)